Prochlorococcus rely on microbial interactions rather than on chlorotic resting stages to survive long-term stress

Dalit Roth-Rosenberg[1]#, Dikla Aharonovich[1]#, Tal Luzzatto-Knaan[1]#, Angela Vogts[2], Luca Zoccarato[3], Falk Eigemann[2], Noam Nago[1], Hans-Peter Grossart[3,4], Maren Voss[2] and Daniel Sher *[1]

[1] Department of Marine Biology, Leon H. Charney School of Marine Sciences, University of Haifa, 31905, Israel; [2] Leibniz-Institute for Baltic Sea Research, Seestrasse15, D-18119 Warnemuende, Germany; [3] Department of Experimental Limnology, Leibniz-Institute of Freshwater Ecology and Inland Fisheries, Alte Fischerhuette 2, D-16775 Stechlin, Germany; [4]Potsdam University, Institute of Biochemistry and Biology, Maulbeeralle 2, D-14469 Potsdam, Germany

* Corresponding author: dsher@univ.haifa.ac.il

# These authors contributed equally to this study

Abstract

Many microorganisms produce resting cells with very low metabolic activity that allows them to survive phases of prolonged stress conditions. Using axenic lab cultures, we show that *Prochlorococcus*, the dominant phytoplankton linage in large regions of the nutrient-poor ocean, cannot survive extended nutrient starvation alone. Under starvation conditions some cells retain metabolic activity, measured as single-cell C and N uptake, but these cultures do not re-grow when transferred into new media. Nevertheless, co-cultures with a heterotrophic bacterium enabled *Prochlorococcus* to survive nutrient starvation for months. We extend these observations to natural conditions, suggesting that up to 10% of the *Prochlorococcus* cells in the oceans live under conditions of light starvation, utilizing organic matter produced by other organisms. We propose that reliance on co-occurring heterotrophic bacteria or on the organic matter they produce, rather than the ability to survive extended starvation as resting cells, underlies the ecological success of *Prochlorococcus*.

Introduction

Not all microbial cells living in natural environments are equally active. In aquatic environments, up to 90% of the cells do not exhibit measurable metabolic activity ("vitality"), based on dyes (e.g. that assess electron transport) or on uptake assays with labeled substrates (Del Giorgio and Gasol 2008). Several

possible and non-exclusive explanations have been proposed for this heterogeneity. First, inherent differences in activity between genetically-different organisms, e.g. due to variations in maximum growth rate or the ability to utilize the specific substrate tested. Second, cells might be at different physiological states, e.g. exponentially growing, starved or dying, and thus less active metabolically(Anderson et al. 2015, Jørgensen et al. 2015, Bergkessel et al. 2016). Third, cells show stochastic fluctuations in their activity, due to noise in gene expression or regulatory networks (Engl 2018). Finally, some organisms respond to environmental stress by producing resting stages or spores. Such cells often exhibit very low (or undetectable) metabolic activity, yet are viable, namely able to return to an active state and reproduce when environmental conditions return to favorable (Harms et al. 2016). The presence of such resting stages, together with a fluctuating activity at the single-cell level and the genetic variability found within natural populations, are suggested to promote the survival of the population as a whole (Lennon and Jones 2011, Bergkessel et al. 2016) .

Understanding the factors affecting the metabolic activity (vitality) of phytoplankton is of special interest. These microbial primary producers perform about one-half of the photosynthesis on Earth, providing energy through carbon fixation at the base of the aquatic ecosystem. At the same time, low nutrient concentrations due to uptake by phytoplankton may constrain the growth of co-occurring organisms. Phytoplankton viability, e.g. their ability to survive under conditions of nutrient stress, has also been extensively studied, especially for organisms that produce massive blooms that emerge and decline rapidly. For example, some bloom-forming cyanobacteria such as *Aphanizomenon* species produce morphologically-distinct spores that show very little photosynthetic activity, yet remain viable in the sediment for long periods of time, providing the inoculum for the next growth season (Sukenik et al. 2015). In laboratory cultures of *Synechococcus elegantus* PCC7942 and *Synechocystis* PCC6803, two unicellular freshwater cyanobacteria, nitrogen starvation results in a programmed process where cells enter a resting stage, enabling them to survive prolonged periods of stress (Sauer et al. 2001, Klotz et al. 2016). As part of this process, cells degrade their photosynthetic apparatus in a controlled manner, resulting in a loss of chlorophyll autofluorescence and culture bleaching (a process termed chlorosis). However, the observation that chlorotic cells are viable resting stages is not universal. Chlorotic cultures of *Microcystis aeruginosa* PCC 7806 were shown to contain a small population of non-chlorotic cells with high chlorophyll autofluorescence (described throughout this study as “high-fl”). Only these high-fl cells were suggested to revive after the re-addition of a nitrogen source, while the low-fl cells are presumably dead (de Abreu Meireles et al. 2015). Chlorotic cells were also observed in eukaryotic phytoplankton

63 albeit it is not yet clear to what extent such cells remain viable as it may depend on the specific
64 organism and stress conditions (Behrenfeld and Falkowski 1997, Franklin et al. 2006).
65 *Prochlorococcus* is a pico-cyanobacterium that is extremely abundant in the oligotrophic
66 oceans, performing an estimated ~8.5% of global ocean photosynthesis (Flombaum et al. 2013), and
67 providing fixed carbon for up to 75% of the co-occurring heterotrophic community (Ribalet et al. 2015).
68 *Prochlorococcus* cells in the oceans exhibit extremely high genetic diversity (Kashtan et al. 2014), and
69 some of this diversity has been linked with their ability to grow under conditions of extreme nutrient
70 limitation (e.g. Martiny et al. 2006, Thompson et al. 2011). It has therefore been suggested that this
71 genetic diversity enables *Prochlorococcus* as a group to thrive across a wide variety of oceanic conditions
72 (Biller et al. 2014). While the physiological and transcriptional responses of multiple *Prochlorococcus*
73 linages to short-term nutrient starvation have been extensively studied (e.g. Steglich et al. 2001, Martiny
74 et al. 2006, Tolonen et al. 2006, Thompson et al. 2011, Krumhardt et al. 2013), little is known about their
75 ability to survive more than a few days under such conditions. A recent study on the response of
76 *Prochlorococcus* strains to extended darkness (i.e. C starvation) has shown that these organisms can
77 survive light starvation only for a limited time (Coe et al. 2016). In these experiments, low-fl cell
78 populations reminiscent of chlorotic cells in other cyanobacteria appear after the light-starved cultures
79 were re-exposed to light, regardless of whether these cultures could continue growing (Coe et al. 2016).
80 We therefore asked: i) Do *Prochlorococcus* respond to long-term nutrient starvation by producing
81 chlorotic cells? ii) If so, are such cells metabolically active (vital) and are they able to reproduce and
82 grow when stress conditions end (viable)? iii) Can chlorotic *Prochlorococcus* cells be observed in nature?
83 To address these questions, we used fluorescence-activated cell sorting (FACS) to obtain distinct
84 chlorotic sub-populations from axenic and unialgal laboratory cultures of *Prochlorococcus* which were
85 pre-incubated with isotopically-labelled tracers for photosynthesis ($H^{13}CO_3$) and nutrient uptake ($^{15}NH_4^+$)
86 and we visualized their activity using Nanoscale Secondary Ion Mass Spectrometry (NanoSIMS). This
87 method enabled us to measure photosynthesis and N uptake at a single cell resolution by quantifying
88 the change in isotopic ratios (Gao et al. 2016, Berthelot et al. 2018). Our results show that while
89 *Prochlorococcus* do undergo a chlorosis-like process, with some of the chlorotic cells still
90 photosynthesizing and taking up NH_4^+, the chlorotic cells are unable to re-grow and thus do not
91 represent resting stages. Instead, co-culture with heterotrophic bacteria in the lab and mixotrophy in
92 the ocean, two aspects of microbial interactions, enable *Prochlorococcus* to survive long-term stress
93 even without producing resting stages.
94

Results and discussion

Emergence of chlorotic sub-populations in *Prochlorococcus* cultures

As *Prochlorococcus* batch cultures reach stationary stage and start declining, the green color of the cultures disappears, and sub-populations of cells emerge with lower chlorophyll autofluorescence that can be identified by flow cytometry (Figure 1A, B). This phenomenon is observed in strains from all major cultured ecotypes, as well as in *Synechococcus* WH8102 (Figure 1C). In *Prochlorococcus* strain MIT9312, lower chlorophyll populations emerged in batch cultures that reached stationary stage due to both N and P limitation, although the timing of sub-population emergence and the forward light scatter and chlorophyll autofluorescence (analyzed by flow cytometry) were different (Supplementary Fig. 1A, B). Cells with lower chlorophyll autofluorescence also appeared in populations of another strain, MIT9313, when these cultures were inhibited in a co-culture with high cell densities of the heterotrophic bacterium *Alteromonas* HOT1A3 (Supplementary Fig. 1C, D (Aharonovich and Sher 2016)). Thus, the emergence of populations of cells with lower chlorophyll autofluorescence under a variety of stress conditions is a pervasive phenomenon across marine pico-cyanobacteria. We therefore focused on *Prochlorococcus* strain MIT9313, which has been extensively studied (e.g. (Rocap et al. 2003, Martiny et al. 2006, Tolonen et al. 2006, Thompson et al. 2011, Voigt et al. 2014)), as in this strain three clearly separate sub-populations can be observed (Figure 1B, referred to throughout the study as high-, mid- and low-fl populations).

In addition to differing in their chlorophyll autofluorescence, the high-, mid- and low-fl cell populations also differ by their forward and side light scatter properties, which are related to cell size and (in larger cells) morphological complexity (Supplementary Fig 2A, B). In agreement with these observations, cells sorted from the high-fl population and observed by SEM (Scanning Electron Microscopy) were larger than those from the mid- and low-fl populations (Sup Fig 2C, D).

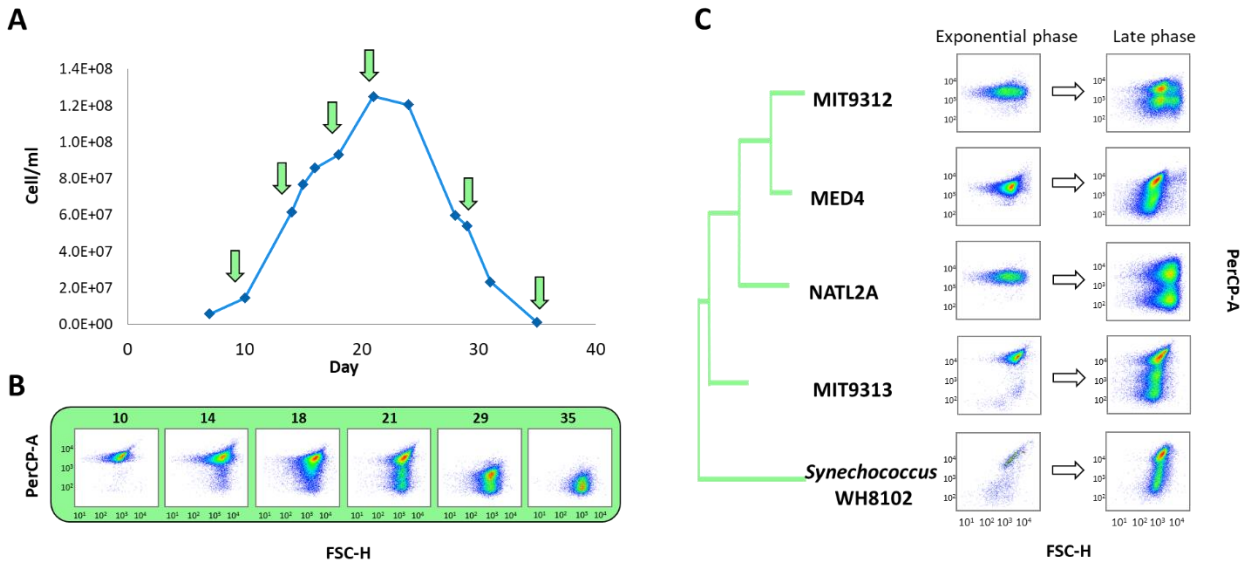

Figure 1. Emergence of chlorotic sub-populations in *Prochlorococcus* batch cultures as measured by flow cytometry. A) A representative growth curve of MIT9313. The arrows mark the days shown in panel B. B) Flow cytometry scattergrams at the marked time-points from the MIT9313 culture. The x-axis is Forward Scatter (FSC, a proxy for cell size), the y-axis is the chlorophyll autofluorescence of the cells (Per-CP). The emergence of chlorotic sub-population observed from the late exponential phase (Day 18). C) Chlorotic sub-population observed in ageing batch cultures of *Prochlorococcus*, belonging to different ecotypes: High-Light adapted MED4 (HLI), MIT9312 (HLII) and Low-Light adapted NATL2A (LLI) and MIT9313 (LLIV). In all strains, the chlorotic cells begin to emerge at late exponential stage, becoming dominant in declining cultures, while in the exponential phase only one population can be observed.

Assessing the metabolic activity of sorted chlorotic sub-populations

We next asked whether the high, mid- and low-fl populations differ in their vitality, measured here as their photosynthesis and nutrient uptake rates (incorporation of $H^{13}CO_3^-$ and $^{15}NH_4^+$, respectively). The uptake ratio of labeled versus unlabeled nutrients were then used to calculate the metabolic activity of the sorted cells (Table 1). As shown in Figure 2 and Table 1, the mean uptake of both $H^{13}CO_3^-$ and $^{15}NH_4^+$ was highest in the high-fl population, followed by the mid and low-fl populations, with the latter population indistinguishable from the control, i.e. glutaraldehyde-killed cells. We have repeated the entire workflow in an independent experiment, and the results are in striking correspondence (Supplementary Fig. 3, Table 1).

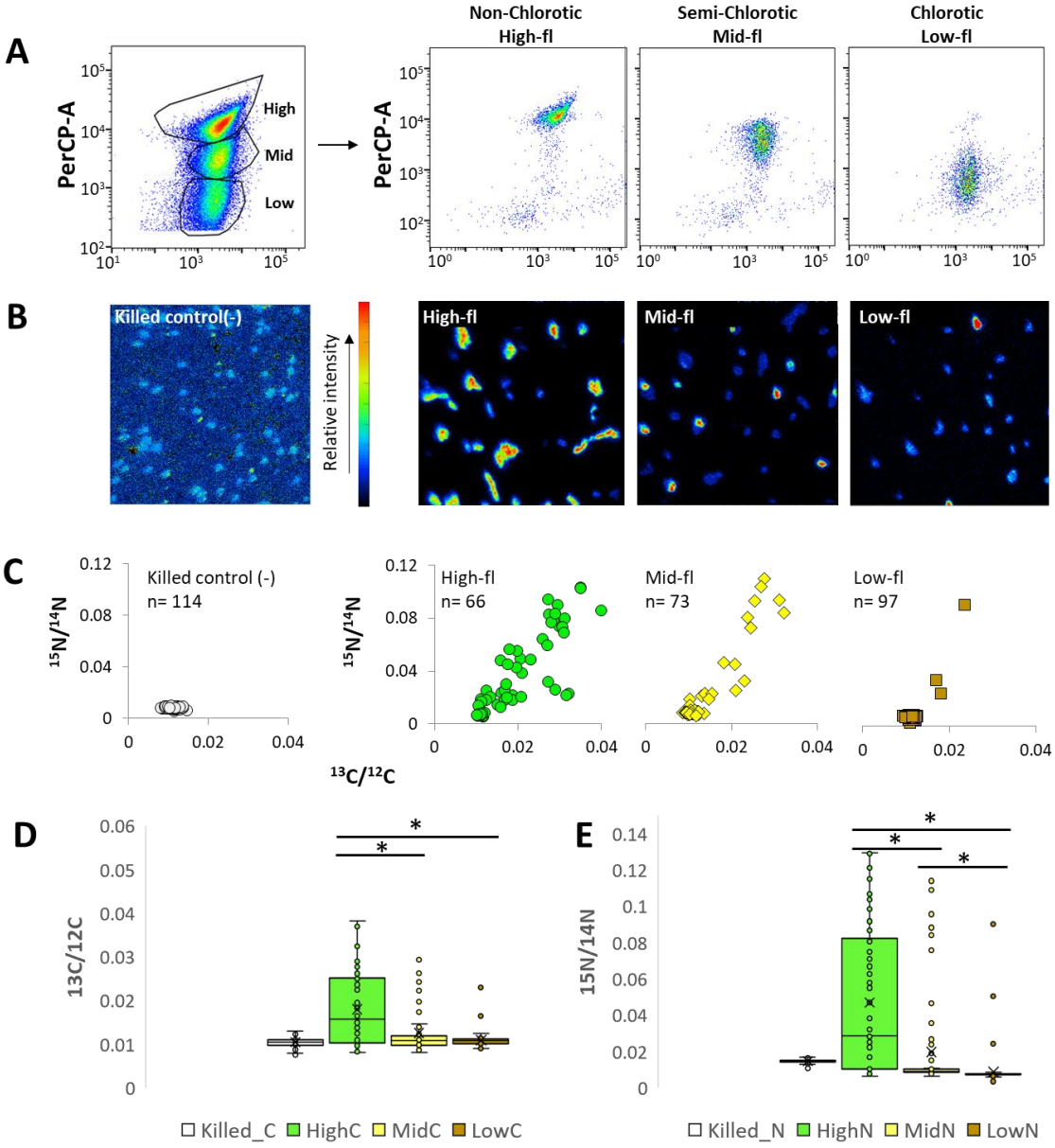

Figure 2. Metabolic activity of sorted sub-populations by NanoSIMS A) Flow cytometry scatterplots before and after sorting of three distinct sub-populations (high, mid and low-fl) of an aging *Prochlorococcus* MIT9313 culture, detected by flow cytometry. The cultures were grown for 30 days in Pro99 and labeled with $H^{13}CO_3^-$ and $^{15}NH_4^+$ for 18h. B) NanoSIMS images of $^{15}N/^{12}C$ analysis of killed cells (negative control) and high, mid and low-fl cells after sorting. C) Scatterplot of $^{13}C/^{12}C$ and $^{15}N/^{14}N$ ratios obtained from NanoSIMS analysis of each sub-population. D, E) Boxplots of the $^{13}C/^{12}C$ and $^{15}N/^{14}N$ enrichment in each sub-population. Lines represent the median, X represents the mean, box borders are 1st quartiles and whiskers represent the full range.

Strain and growth stage	Sub-population	Illumination	V^C (fg cell^{-1} day^{-1})	V^N (fg cell^{-1} day^{-1})
Batch culture				
MIT9313, exponential growth*	High	Constant light 27 µE	12.92 ± 11.93	2.74 ± 2.43
MIT9313, old cultures **	High	Constant light 27 µE	2.67-2.77 ± 2.89-3.57	0.62-0.69 ± 0.54-0.63
	Mid		0.75-0.79 ± 1.73-1.78	0.25-0.32 ± 0.42-0.35
	Low		0.09-0.14 ± 0.52-0.67	0.08-0.14 ± 0.15-0.12
MIT9313, old culture***	High	Photo-period 12:12 L/D, 27 µE	1.01 ± 2.67	0.32 ± 0.33
	Mid		0.48 ± 2.47	0.20 ± 0.20
	Low		0.13 ± 0.31	0.14 ± 0.11
Natural samples				
115m	High	Natural cycle approximately 14:10 L/D, 2-5 µE	1.04 ± 0.6	1.17 ± 0.20
115m	Low		1.14 ± 0.69	1.15 ± 0.38
125m	High		1.21 ± 0.89	1.28 ± 0.21

Table 1: Calculated mean C and N uptake rates from the experiments performed with *Prochlorococcus* MIT9313 and natural samples. The means and standard deviation were calculated from the uptake rates values of single cells in each experiment.

*The results for MIT9313 exponential growth refers to the experiment presented in Supplementary Fig. 5.

**The results for old MIT9313 cultures under constant light refer to the two experiments presented in Fig. 2 and Supplementary Fig. 3.

*** The results for Old MIT9313 cultures under L/D refer to the experiment presented in Supplementary Fig. 4.

The mean uptake rates for glutaraldehyde killed cells (control) were 0.06±0.15 for C and 0.18±0.02 for N, and most likely depict the absorption of the label by non-specific binding or diffusion. Unlabeled-unsorted cells showed C values of 0.18±0.39.57 and N values of 0.41±0.14, the higher C and N values were probably due to non-sorted conditions and the higher density of the cells.

Within each of the populations, cell-cell heterogeneity was observed in both ^{13}C and ^{15}N uptake (Fig. 2, Supplementary Fig. 3). Within all of the populations (including the high-fl, "healthy" one), some cells were inactive, and this could not be explained by the limited purity of the FACS-sorting procedure

(Supplementary Tables 1,2). The coefficients of variation in C and N uptake rates were within the range shown for other organisms, or higher (Supplementary Table 3, (Matantseva et al. 2016, Berthelot et al. 2018)). Similar levels of heterogeneity (primarily in N uptake) were also seen in cells grown under a 12:12 light-dark cycle, where the *Prochlorococcus* cell-cycle follows a diel rhythm, suggesting that this heterogeneity is not due to different stages of the cell cycle or the diel cycle (Supplementary Table 3, Supplementary Fig. 4). Cell-cell heterogeneity was also observed in cells from an exponentially-growing, nutrient-replete culture (Supplementary Figure 5, Table 3), suggesting that this heterogeneity is not exclusively limited to ageing or stressed cells. This is in accordance with studies assessing the vitality of *Prochlorococcus* cells using various dyes, which consistently show that a significant fraction of the cells in laboratory cultures are inactive or potentially dead (Agusti and Sanchez 2002, Hughes et al. 2011).

Evaluating the viability of sub-populations

To determine whether the low-fl *Prochlorococcus* cells are viable resting stages, we tested the ability of cells from an MIT9313 culture to grow upon transfer to new growth media at different times during exponential growth and upon culture decline. As shown in Figure 3 and Supplementary Fig. 6, only cells from cultures where the high-fl cells were dominant could grow when transferred to new growth media. No growth was observed upon transfer of cells from stationary or declining cultures where no high-fl cells were observed. Intriguingly, the presence of high-fl cells was not enough to ensure culture growth (e.g. day 34 in Figure 3). This is consistent with a previous study showing that cells belonging to a different *Prochlorococcus* strain, MED4, that were incubated for three days in the dark, were unable to resume growth after return to light despite showing no clear difference in the chlorophyll autofluorescence (Coe et al. 2016). The probability of growth after transfer did not depend on the number of transferred cells (Morris et al. 2008), with as many as 2.5×10^7 cells/ml failing to grow after transfer during culture decline (cells at ~1/10 of this density grew after being transferred during exponential stage). Thus, non-chlorotic cells (defined as being within the range of chlorophyll autofluorescence exhibited by exponentially-growing cells) are not necessarily viable.

As shown in Figure 4, the inability to survive prolonged nitrogen starvation is not unique to MIT9313, but rather is common to the four tested *Prochlorococcus* strains, covering the major cultured ecotypes. This is in marked contrast to the ability of (presumably axenic) cultures of two freshwater cyanobacteria, *Synechococcus* PCC 7942 and *Synechocystis* PCC 6803, to revive after extended N starvation (Sauer et al. 2001, Klotz et al. 2016). However, when co-cultured with a heterotrophic

bacterium, *Alteromonas* HOT1A3, all *Prochlorococcus* strains were able to re-grow after 60 days of N stress. Interestingly, strain MIT9313, which was initially inhibited by this *Alteromonas* strain (Figure 4A, (Sher et al. 2011, Aharonovich and Sher 2016)), was also able to survive long-term starvation in co-culture, suggesting that fundamentally different interactions occur during exponential growth compared to long-term, presumably nutrient-limited growth. These results are consistent with the ability of heterotrophic bacteria to extend the survival time of different *Prochlorococcus* strains under conditions

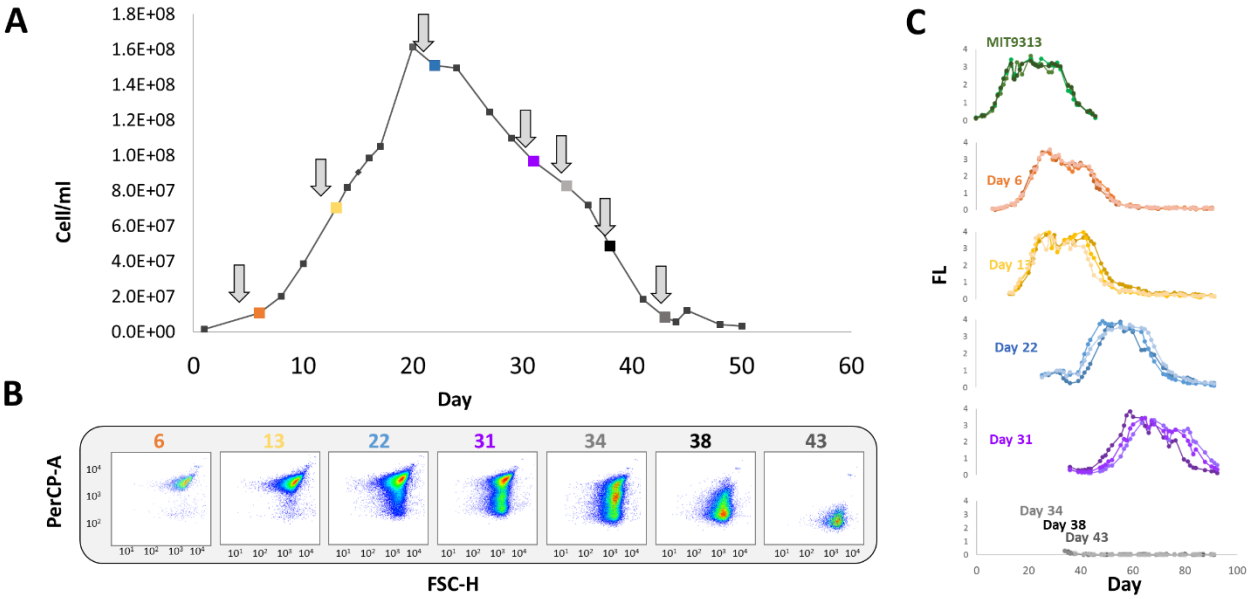

of constant darkness (albeit for only several days, (Coe et al. 2016)) and with the ability of different heterotrophic bacteria to support the long-term viability of batch cultures of *Synechococcus* WH7803 (Christie-Oleza et al. 2017).

Figure 3: Time-dependent changes in viability of cells transferred into fresh media at different life cycle stages of a batch culture. A) Growth curve of an MIT9313 culture, grown in Pro99, similar to the experiments shown in Figure 2 and Supplementary Fig. 3, 4 and 7. Arrows indicate the time points at which triplicate 1ml samples were transferred into fresh media. B) Flow cytometry scatterplots of the culture shown in panel A. C) Growth curves of cells being transferred at different times to new, nutrient-replete media (assessed via bulk culture fluorescence). Cells could not re-grow when transferred after day 34, suggesting that not all high-fl cells are viable, and that mid- and low-fl cells are non-viable.

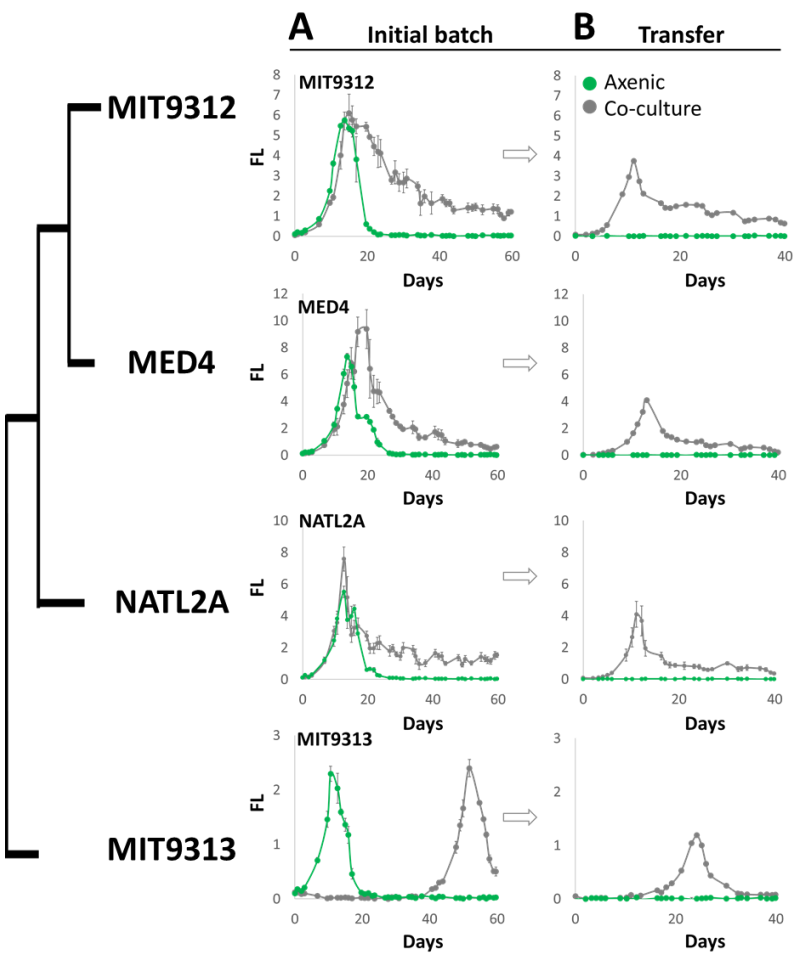

Figure 4: Co-culture with a heterotrophic bacterium, *Alteromonas* HOT1A3, enables multiple *Prochlorococcus* strains to survive long-term N starvation. Panel A: 10^6 axenic *Prochlorococcus* cells/ml from different strains were incubated alone (green line) or with the addition of 10^7 *Alteromonas* HOT1A3 cells/ml in low-N media (grey line). Bulk culture fluorescence was recorded as a proxy for cell growth, and 1ml from each culture was transferred into fresh media after 60 days. Panel B: The transferred cultures were recorded for additional 40 days. Error bars are standard deviation from triplicate cultures. The late growth of MIT9313 in co-culture is the "delayed growth" phenotype described in (Sher et al. 2011, Aharonovich and Sher 2016).

Exploring the metabolic activity of naturally occurring sub-populations of *Prochlorococcus* at different depths in the eastern Mediterranean

While chlorotic cells consistently emerge under nutrient starvation in all tested *Prochlorococcus* strains (Fig 1), environmental conditions in laboratory cultures greatly differ from those in the oligotrophic sea. For example, cell densities and nutrient concentrations are typically orders of magnitude higher in the lab than in the nutrient-poor ocean. Indeed, little is known about the prevalence of chlorosis under natural conditions for phytoplankton in general. Thus, we wondered whether chlorotic *Prochlorococcus* cells (defined as low-fl and low C and N uptake) can be identified also in nature. We focused on the deep euphotic zone (100-140m, above the nutricline) where both inorganic nutrient concentrations and light availability are low. At this depth, "double" *Prochlorococcus* populations, differing by their chlorophyll auto-fluorescence, have repeatedly been observed (e.g. (Campbell and Vaulot 1993, Moore et al. 1998)). Previously, these double populations have been shown to contain genetically-different cells belonging to the High-Light adapted (HL, low chlorophyll) and Low-Light adapted (LL, high chlorophyll) clades (Moore et al. 1998), However, a recent study using genetic tools suggested that each of the double populations consists of both HL and LL cells, implying that phenotypic heterogeneity (acclimation) can also contribute to this phenomenon (Thompson et al. 2018). We therefore asked whether the double population could also be due to the presence of chlorotic cells, e.g. if LL cells were mixed above the nutricline, became exposed to nutrient starvation, and subsequently underwent chlorosis. To test this hypothesis, we characterized the *Prochlorococcus* population structure and single-cell activity (carbon fixation and NH_4^+ uptake) during late summer in the ultra-oligotrophic Eastern Mediterranean Sea (Figure 5A, B). At the time of sampling, the water column was highly stratified and nutrients were depleted down to around 130m, with a peak in NH_4^+ concentrations slightly above the nutricline (15nM at 115m and 125m, Fig. 5B). *Prochlorococcus* were the numerically dominant phytoplankton (Fig 5C), exhibiting a double population at 115m, but not at samples collected above or below this depth (Fig 5E). Amplicon sequencing of the Internal Transcribed Spacer between the 16S and 23S genes (ITS, (Thompson et al. 2018)) revealed that between ~100-137m LL cells (belonging primarily to the LL-I and LL-IV clades) gradually replace the HL cells, consistent with previous studies (e.g. (Malmstrom et al. 2010)) but contrasting with the sharp delineation between high-chlorophyll and low-chlorophyll *Prochlorococcus* populations (Fig. 5E, (Thompson et al. 2018)).

Mean $H^{13}CO_3^-$ and $^{15}NH_4^+$ uptake rates for the majority of the cells sorted from each of the double *Prochlorococcus* populations at 115m depth were not statistically different, nor were they

different from cells collected at greater water depths (Figure 5. F, G, Kruskal-Wallis test, p=0.7 for C and p=0.07 for N). Essentially all of the cells from the Eastern Mediterranean were active, although we did observe some cells with lower C and N uptake rates in the low-fl population at 115m depth (6/45 cells, Figure 5F). This contrasts with the observation from our lab experiments, where inactive cells were observed in all populations, and formed the majority of the cells in the chlorotic (mid- and low-fl) populations. The observation that essentially all of the *Prochlorococcus* cells in natural samples are active is consistent with a similar study in the North Pacific (Berthelot et al. 2018).

At a depth of 115m light intensity was low (5-6μE during the afternoon), potentially enough to support the growth of some LL strains but not sufficient for active growth under laboratory conditions of most HL strains, including those that are present based on the ITS sequences (Moore and Chisholm 1999). However, previous studies based on cell cycle analysis and on ^{14}C incorporation into divinyl-chlorophyll a have suggested that, even at this depth, *Prochlorococcus* cells divide every 4-7 days (Goericke and Welschmeyer 1993, Vaulot et al. 1995, Binder et al. 1996, Partensky et al. 1996). The C uptake rates observed in the cells from 115 and 137m were well below the rate required to support this division rate (~1 fg cell^{-1} day^{-1}, Table 1). Additionally, unlike the laboratory cultures, in which C incorporation rates were 3-6 times larger than N-incorporation rates, in our samples from the Mediterranean Sea the measured C:N uptake ratio was about 1. Thus, the measured C and N uptake rates suggest that, most likely, *Prochlorococcus* obtain most of the carbon needed for cell growth from non-photosynthetic sources, i.e. through mixotrophy.

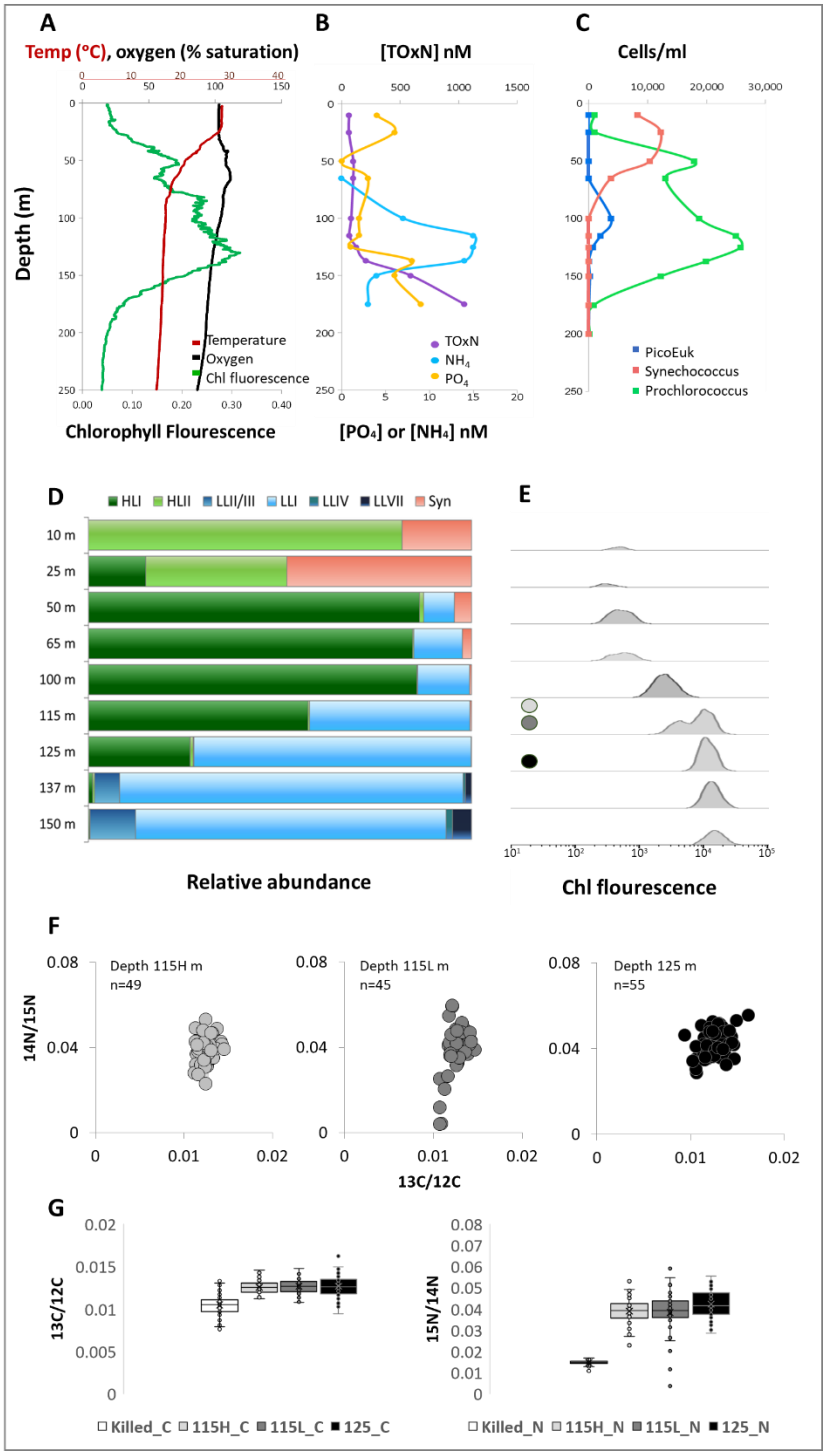

Figure 5: Nutrient uptake of naturally occurring *Prochlorococcus* populations at the Eastern Mediterranean Sea. A-C) Oceanic parameters at the sampling site: Temperature, Oxygen and

Chlorophyll (A); Nutrient concentrations (B); Cell counts by flow cytometry (C). D) Relative abundance of different *Prochlorococcus* clades across the water column, determined by ITS sequencing. E) Histograms of chlorophyll autofluorescence, analyzed from flow cytometry of picoplankton throughout the water column. Note the double population at 115m. F) Scatterplot of $^{13}C/^{12}C$ and $^{15}N/^{14}N$ ratios obtained from NanoSIMS analysis of each sorted sub-population from 115m and the single population from 125m. G) Boxplots of the $^{13}C/^{12}C$ and $^{15}N/^{14}N$ enrichment in each sub-population. Lines represent the median, X represents the mean, box borders are 1st quartiles and whiskers represent the full range. The three populations did not statistically differ (Kruskal-Wallis test, $p<0.001$).

Stress survival in pico-cyanobacteria: why is *Prochlorococcus* different?

In this study, we demonstrate that phenotypic heterogeneity between clonal *Prochlorococcus* cells occurs at multiple "scales". In exponentially growing axenic laboratory cultures C and N uptake rates differ significantly between individual cells. This variation is independent of genetic variability. Additionally, as axenic cultures become stressed, a larger phenotypic change occurs as cells lose their chlorophyll auto-fluorescence and become chlorotic. Under these experimental conditions, most cells are inactive (primarily in the low-fl population), although, due to the level of sensitivity of the NanoSIMS, we cannot rule out that even low-fl cells still retain a residual level of activity. Some cells from the chlorotic populations retain at least part of their photosynthetic capacity, and indeed can fix carbon and take up NH_4. Yet, in our experiments, they do not re-grow when condition become more favorable. In *Synechococcus elegantus* PCC 7942, chlorotic cultures retain approximately 0.01% of their photosynthetic activity, as well as a residual level of protein translation, although it remains unclear whether this is a process shared by all cells in the culture or whether this activity is only due to a small subset of more active cells (Sauer et al. 2001). The clear difference between the ability of axenic *Synechococcus elegantus* PCC 7942 and *Synechocystis* PCC6803 to survive long-term N starvation, and the inability of axenic *Prochlorococcus* cultures to do so, suggests an inherent difference in the physiology and genomic functional capacity between these unicellular cyanobacteria.

Entry into chlorosis in *Synechocystis* is a regulated process that involves the organized degradation of the phycobilisomes in parallel with an increase in the storage products glycogen and polyhydroxybutyrate (PHB) (Klotz et al. 2016). The photosynthesis apparatus of *Prochlorococcus* is different from that of other cyanobacteria, using unique chlorophyll a2/b2 binding proteins rather than phycobilisomes (Ting et al. 2002), and indeed they lack orthologs of the nblA gene required for

phycobilisome degradation during chlorosis (Klotz et al. 2016). Additionally, while *Prochlorococcus* likely use glycogen as a C storage pool (Lichtlé et al. 1995), they lack the phaA-C and phaE genes required for PHB biosynthesis and which are induced in *Synechocystis* PCC 6803 under chlorosis (although these genes are not required for revival from chlorosis (Klotz et al. 2016)). Taken together, these differences suggest that *Prochlorococcus* lack the genetic toolkit employed by *Synechocystis* PCC6803 and *Synechococcus elegantus* PCC7942 to enter into a resting stage.

If *Prochlorococcus* are indeed incapable of producing resting stages in response to nutrient or light starvation, what are the evolutionary drivers of this phenotype, and what are the consequences for the dynamics of *Prochlorococcus* populations in the ocean? While the open oligotrophic ocean is often considered a relatively stable environment, nutrient concentrations do fluctuate, and phytoplankton (including *Prochlorococcus*) inhabiting these waters show multiple signs of nutrient stress (Moore et al. 2013, Saito et al. 2014). Many of the microbes that live in such environments comprising a large fraction of the surface ocean have small, highly streamlined genomes (Yooseph et al. 2010) and this has been suggested to be an adaptation to low nutrient concentrations (Yooseph et al. 2010, Biller et al. 2014, Giovannoni 2017). It is possible that the lack of resting stages is a result of this genome streamlining (the genomes of *Synechococcus elegantus* PCC7942 and *Synechocystis* PCC6803 are ~3.2mbp and ~4mbp with their plasmids, respectively, compared to ~1.4-2.5 mbp for *Prochlorococccus* strains).

Surviving nutrient stress "with a little help from my friends".

Despite the clear effect of nutrient stress on *Prochlorococcus* in laboratory culture, manifesting in chlorosis and reduction of vitality, we observed relatively few less-active (potentially chlorotic) *Prochlorococcus* cells in the deep euphotic zone of the Eastern Mediterranean (approximately 5% of the population at 115m, Figure 5F). It is possible that cell stress and chlorosis change as a function of the diel cycle, and indeed previous studies have suggested *Prochlorococcus* cell mortality increases during the night (Llabrés et al. 2011, Ribalet et al. 2015). As the sampling of natural population in the Eastern Mediterranean Sea took place during the day (~12:00-16:00) we cannot exclude this hypothesis. Alternatively, *Prochlorococcus* may actually never experience nutrient starvation in the oceans. While physiological and molecular analyses of field populations of Prochlorococcus suggest that the cells are nutrient-limited (e.g. (Saito et al. 2014, Szul et al. 2019)), cell growth and death are usually balanced, suggesting these cells are not experiencing acute starvation (e.g. (Ribalet et al. 2015)). The ability of *Prochlorococcus* to thrive under conditions of extreme nutrient limitation is often explained by their

small cell size (increasing their biomass-specific diffusion), their generally low nutrient requirements, and their specific metabolic strategies to minimize the per-cell elemental quotas (Van Mooy et al. 2006, Gilbert and Fagan 2011, Read et al. 2017). We propose that interactions with co-occurring microorganisms, e.g. through the recycling of inorganic nutrients or the exchange of organic compounds, enable *Prochlorococcus* to survive when these nutrient-saving mechanisms are not sufficient. Indeed, the observation that *Prochlorococcus* can compete with heterotrophic bacteria for amino acids (Zubkov et al. 2004), carbohydrates (Muñoz-Marín et al. 2013) and perhaps DMSP (Vila-Costa et al. 2006, Becker et al. 2019) suggests that mixotrophy is prevalent and important in natural communities. This is supported by genomic analyses (Rocap et al. 2003, Yelton et al. 2016). The importance of mixotrophy is not limited to organic forms of N, P or Fe, but can be extended to light (or resulting C) stress. Illustrating the potential magnitude of this effect, an average of ~8-10% of the *Prochlorococcus* cells at HOT and BATS (Hawaii and Bermuda time series study sites, respectively (Malmstrom et al. 2010)), are found under conditions where the average integrated illumination is not enough to support their growth under laboratory conditions (Sup Fig. S7, see supplementary text for more details (Moore and Chisholm 1999)). This includes the vast majority of LL adapted ecotypes. Previous studies have shown that uptake of glucose by *Prochlorococcus* cells in the central Atlantic Ocean can support up to ~20% of their carbon requirements, supporting the notion of mixotrophy (Muñoz-Marín et al. 2013, Muñoz-Marín et al. 2017). However, glucose uptake is light dependent and occurs at higher rates in the surface ocean, suggesting that some other form of DOC is likely important in the deep euphotic zone. Amino acids provide another potential DOC form, which can supply both N and C to the cells. Indeed, cell-specific amino acid uptake rates of *Prochlorococcus* from the southern Atlantic Ocean increase with depth, and high-fl cells take up more than low-fl cells, although to what extent this supports the C and N needs of the cells is unknown (Zubkov et al. 2004). Regardless of the specific forms of dissolved organic carbon being utilized by the cells, the lack of any mechanism for the production of resting stages by *Prochlorococcus* may be considered another manifestation of the "Black Queen Hypothesis", which states that microorganisms "outsource" essential survival mechanisms such as detoxification of reactive oxygen species to the surrounding microbial community (Morris et al. 2012). These forms of microbial interactions likely affect the distribution and activity of *Prochlorococcus* on a global scale (Hennon et al. 2017, Ma et al. 2017).

Material and Methods

Prochlorococcus growth and Stable Isotope Incubations

Axenic *Prochlorococcus* strains were grown in Pro99 media under constant cold while light (27 µE) at 22 °C. Bulk chlorophyll fluorescence (FL) (ex440; em680) was measured almost daily using a Fluorescence Spectrophotometer (Cary Eclipse, Varian). In parallel, samples for flow cytometry were taken for cell numbers. When three distinct sub-populations appeared in the flow cytometry, the cultures were labeled with 1mM Sodium bicarbonate-^{13}C and 1mM Ammonium-^{15}N chloride (Sigma-Aldrich, USA) for 18-24 hours. The optimal incubation time based on preliminary isotope labeling experiments with Prochlorococcus MED (Supplementary figure 8). Incubations were stopped by fixing 2 ml of the culture with 2X EM grade glutaraldehyde (2.5% final concentration) and subsequently storing at 4 °C until the sorting analysis. Non-labeled cells that were killed before labeling (by adding 2.5% glutaraldehyde) were used as a negative control.

Cell Sorting and Filtration

Sorting of sub-population was carried out using a BD FACSAria III sorter (BD Biosciences) at the Life Sciences and Engineering Infrastructure Center, Technion, Israel. Each sample was sorted for 3 sub-populations: Non-chlorotic (High-fl), Semi chlorotic (Mid-fl) and Chlorotic (Low-fl) (Figure 2A). The sorting gates for each sub-population were determined from the population observed in forward scatter (FSC, a proxy for cell size) and auto-fluorescence (PerCP, chlorophyll auto-fluorescence). After sorting, the sorted sup-population were gently filtered on 13 mm diameter polycarbonate filters (GTTP, 0.2 µM pore size, Millipore, MA), washed twice with sterile sea water and air-dried. The filters were stored at 4 ºC until nanoSIMS analyses.

Nanoscale secondary ion mass spectrometry (nanoSIMS) and data analysis

The samples were coated with a layer of ca. 30 nm gold with a Cressington 108 auto sputter coater (Watford, United Kingdom). Random spots were employed for NanoSIMS analyses. SIMS imaging was performed using a NanoSIMS 50L instrument (Cameca, Paris, France) at the Leibniz-Institute for Baltic Sea Research Warnemünde (IOW). A $^{133}Cs^+$ primary ion beam was used to erode and ionize atoms of the sample. Images of secondary electrons, $^{12}C^-$, $^{13}C^-$, $^{12}C^{14}N^-$ and $^{12}C^{15}N^-$ were recorded simultaneously using mass detectors equipped with electron multipliers (Hamamatsu). The mass resolving power was adjusted to be sufficient to suppress interferences at all masses allowing, e.g. the separation of $^{13}C^-$ from interfering ions such as $^{12}C^1H^-$. Prior to the analysis, sample areas of 50×50 µm were sputtered for 2 min

434 with 600 pA to erode the gold, clean the surface and reach the steady state of secondary ion formation.
435 The primary ion beam current during the analysis was 1 pA; the scanning parameters were 512×512
436 pixels for areas of 30x30 to 48x48 µm, with a dwell time of 250 µs per pixel. 60 planes were analysed.
437

438 **Analyses of NanoSIMS measurements**

439 All NanoSIMS measurements were analysed with the Matlab based program look@nanosims (Polerecky
440 et al., 2012). Briefly, the 60 measured planes were checked for inconsistencies and all usable planes
441 accumulated, regions of interest (ROI's) (i.e. Prochlorococcus cells and filter regions without organic
442 material for background measurements) defined based on $^{12}C^{14}N$ mass pictures, and $^{13}C/^{12}C$ as well as
443 $^{12}C^{15}N/^{12}C^{14}N$ ratios calculated from the ion signals for each region of interest.

444 **Uptake rate calculation**

445 Uptake rate was estimated using the following equation, based on that of (Legendre and Gosselin 1997),
446 as follows:

447 $$V = \frac{(\%P_t^* - \%P_0^*)}{(\%D_i^* - \%D_0^*)} \frac{Q}{t}$$

448 Where $\%P^*_t$ is the concentration (atom %) of the heavy isotope in the particulate matter at the end of
449 the incubation, $\%D^*_i$ is the concentration of the dissolved tracer added to the incubation (and assumed
450 not to change over the short incubation time), and $\%P^*_0$ and $\%D^*_0$ are the natural heavy isotope
451 concentrations in the particulate and dissolved matter, respectively. We estimated *Q*, the cell quota (in
452 fg cell^{-1}) of C or N, based on measurements of the biomass of MED4 and MIT9313 (66 fg cell^{-1}and 158 fg
453 cell^{-1}, respectively, (Cermak et al. 2016)) and assuming that C comprises 50% and N comprises 7.5% of
454 the cell biomass. For heavy isotopes concentration in the particulate and dissolved phases before
455 incubation we used the natural values for isotopic ratios of ^{13}C and ^{15}N (1.12% and 0.37% respectively).
456 For the experiment shown in Supplementary Fig. 8, we measured the NH_4^+ concentration in the media
457 and added the ^{15}N tracer to 50% final concentration. Since all other experiments were performed in
458 declining cultures we assumed that the NH_4^+ was depleted from the media, and thus $\%D^*_t$ was defined
459 as 90%, based on previous measurements of NH_4^+ concentrations in old cultures. We used a value of
460 50% for the initial percentage of ^{13}C, based on dissolved inorganic carbon (DIC) measurements
461 (Grossowicz et al. 2017). For the terminal concentrations of ^{15}N and ^{13}C in the particulate phase ($\%P^*_t$) we
462 used the values of $^{13}C/^{12}C$ and $^{15}N/^{14}N$ that were obtained from the NanoSims analysis of the cells.

463 $^{13}C/^{12}C$ and $^{15}N/^{14}N$ below the natural values resulted with negative uptake values, and were treated as
464 zero uptake.

465 Mean and standard deviation of C and N uptake rates were calculated from the uptake rate values of
466 individual cells (Table 1). The uptake rate values were not corrected for negative control (killed cells),
467 which are presented for comparison in table 1. Since $^{13}C/^{12}C$ and $^{15}N/^{14}N$ values of individual cells were
468 not normally distributed, for significance analysis we used non-parametric tests (Mann-Whitney and
469 Kruskal-Wallis tests) performed using the Real Statistics Resource Pack software (Release 5.4 www.real-
470 statistics.com).

471 **Isotope labelling and phylogenetic analysis of a natural marine bacterioplankton population at sea**
472 **Water collection and labelling experiment procedure**
473 Mediterranean seawater was collected during August 2017 (station N1200, 32.45 degrees N, 34.37
474 degrees E) from 11 depths by Niskin bottles and divided into triplicates of 250 ml polycarbonate bottles.
475 Two bottles from each depth were labeled with 1mM Sodium bicarbonate-^{13}C and 1mM Ammonium-^{15}N
476 chloride (Sigma-Aldrich, USA) and all 3 bottles (2 labelled and 1 control) were incubated at the original
477 depth and station at sea for 3.5 hours on day time. After incubation, bottles were brought back on board
478 and the incubations were stopped by fixing with 2X EM grade glutaraldehyde (2.5% final concentration)
479 and stored at 4 °C until sorting analysis.
480
481 **DNA collection and extraction from seawater**
482 Samples for DNA collected on a 0.22 µm sterivex filters (Millipore). Excess water was removed using a
483 syringe and 1 ml Lysis buffer (40 mM EDTA, 50 mM Tris pH 8.3, 0.75 M sucrose) was added and both
484 ends were closed with parafilm. Samples were kept at -80°C until extraction. DNA extracted by using a
485 semi-automated protocol includes manually chemical cell lysis before the automated steps. The manual
486 protocol began with thawing the samples, then the storage buffer was removed using a syringe and 170
487 µl lysis buffer added to the filter. 30 µl of Lysozyme (20 mg/ml) added to filters and incubate at 37°C for
488 30 min. After incubation, 20 µl proteinase K and 200 µl Buffer AL added to the tube for 1 hour at 56°C
489 (with agitation). Then, the supernatant transferred to a new tube, which subjected to the QIAcube
490 automated system (at the BioRap unit, Faculty of Medicine, Technion) following the manufacturer's
491 instructions using QIAamp DNA Mini Protocol: DNA Purification from Blood or Body Fluids (Spin
492 Protocol) from step 6. All DNA samples were eluted in 100 µl DNA free distilled-water.
493

494 **16S and ITS PCR amplification**

495 PCR amplification of the ITS was carried out with specific primers for *Prochlorococcus* CS1_16S_1247F
496 (5'-ACACTGACGACATGGTTCTACACGTACTACAATGCTACGG) and Cs2_ITS_Ar (5'-
497 TACGGTAGCAGAGACTTGGTCTGGACCTCACCCTTATCAGGG) (Thompson et al. 2018). The first PCR was
498 performed in triplicate in a total volume of 25 µl containing 0.5 ng of template, 12.5 µl of MyTaq Red
499 Mix (Bioline) and 0.5 µl of 10 µM of each primer. The amplification conditions comprised steps at 95°C
500 for 5 min, 28/25 (16S/ITS) cycles at 95°C for 30 sec, 50°C for 30 sec and 72°C for 1 min followed by one
501 step of 5 min at 72°C. All PCR products validated on 1% agarose gel and triplicates were pooled.
502 Subsequently, a second PCR amplification was performed to prepare libraries. These were pooled and
503 after a quality control sequenced (2x250 paired-end reads) using an Illumina MiSeq sequencer. Library
504 preparation and pooling were performed at the DNA Services (DNAS) facility, Research Resources Center
505 (RRC), University of Illinois at Chicago (UIC). MiSeq sequencing was performed at the W.M. Keck Center
506 for Comparative and Functional Genomics at the University of Illinois at Urbana-Champaign (UIUC).
507
508 **ITS Sequence processing** Paired-end reads, in the format of fastq files were analyzed by the DADA2
509 pipeline (https://www.nature.com/articles/nmeth.3869). Quality of the sequences per sample was
510 examined using the Dada2 'plotQualityProfile' command. Quality filtering was done using the Dada2
511 'filterAndTrim' command with parameters for quality filtering were truncLen=c(290,260), maxN=0,
512 maxEE=c(2,2), truncQ=2, rm.phix=TRUE, trimLeft=c(20,20). Following error estimation and dereplication,
513 the dada algorithm was used to correct sequences. Merging of the forward and reverse reads was done
514 with minimum overlap of 4 bp. Detection and removal of suspected chimera was done with command
515 'removeBimeraDenovo'. In total, 388,417 sequences in 484 amplicon sequence variants (ASVs) were
516 counted. The ASVs were aligned in MEGA6 (Tamura et al. 2013) and the first ~295 nucleotides,
517 corresponding to the 16S gene, were trimmed. The ITS sequences were then classified using BLAST
518 against a custom database of ITS sequences from cultured Prochlorococcus and Synechococcus strains
519 as well as from uncultured HL and LL clades.

520 **Acknowledgements**

521 We thank the captain and crew of the R/V Mediterranean Explorer and Tom Reich, for help during the
522 work at sea, Maya Lalzar for assistance with the bioinformatics analysis and Annett Grüttmüller
523 NanoSIMS routine operation. This study was supported by grant RGP0020/2016 from the Human
524 Frontiers Science Program (to MV, HPG and DS) and by grant number 1635070/2016532 from the NSF-

BSF program in Oceanography (NSFOCE-BSF, to DS). The NanoSIMS at the Leibnitz-Institute for Baltic Sea research in Warnemuende (IOW) was funded by the German Federal Ministry of Education and Research (BMBF), grant identifier 03F0626A.

Author contributions

DRR, DA, TLK, AV, MV and DS designed experiments, DRR, DA, TLK, LZ, NN and DS performed experiments and field analyses, DRR, DA, TLK, AV, and FE performed NanoSIMS analyses, DRR, DA, TLK, AV, LZ, FE, NN, HPG, MV and DS analyzed results, DRR, DA, TLK and DS wrote manuscript with contributions from all authors.

Competing interests

The authors declare no competing interests

Materials and Correspondence

Please send requests for materials or other correspondence to Daniel Sher, dsher@univ.haifa.ac.il

References:

Aharonovich, D. and D. Sher (2016). "Transcriptional response of Prochlorococcus to co-culture with a marine Alteromonas: differences between strains and the involvement of putative infochemicals." ISME J **10**(12): 2892-2906.

Anderson, T. R., J. R. Christian and K. J. Flynn (2015). Chapter 15 - Modeling DOM Biogeochemistry. Biogeochemistry of Marine Dissolved Organic Matter (Second Edition). D. A. Hansell and C. A. Carlson. Boston, Academic Press**:** 635-667.

Barton, A. D., S. Dutkiewicz, G. Flierl, J. Bragg and M. J. Follows (2010). "Patterns of diversity in marine phytoplankton." Science **327**(5972): 1509-1511.

Becker, J. W., S. L. Hogle, K. Rosendo and S. W. Chisholm (2019). "Co-culture and biogeography of Prochlorococcus and SAR11." The ISME Journal.

Behrenfeld, M. J. and P. G. Falkowski (1997). "Photosynthetic rates derived from satellite-based chlorophyll concentration." Limnology and Oceanography **42**(1): 1-20.

Bergkessel, M., D. W. Basta and D. K. Newman (2016). "The physiology of growth arrest: uniting molecular and environmental microbiology." Nature Reviews Microbiology **14**: 549.

Berthelot, H., S. Duhamel, S. L'Helguen, J.-F. Maguer, S. Wang, I. Cetinić and N. Cassar (2018). "NanoSIMS single cell analyses reveal the contrasting nitrogen sources for small phytoplankton." The ISME Journal.

Biller, S. J., P. M. Berube, D. Lindell and S. W. Chisholm (2014). "Prochlorococcus: the structure and function of collective diversity." Nature Reviews Microbiology **13**: 13.

Binder, B. J., S. W. Chisholm, R. J. Olson, S. L. Frankel and A. Z. Worden (1996). "Dynamics of picophytoplankton, ultraphytoplankton and bacteria in the central equatorial Pacific." Deep Sea Research Part II: Topical Studies in Oceanography **43**(4): 907-931.

564 Campbell, L. and D. Vaulot (1993). "Photosynthetic picoplankton community structure in the subtropical
565 North Pacific Ocean near Hawaii (station ALOHA)." Deep Sea Research Part I: Oceanographic Research
566 Papers **40**(10): 2043-2060.
567 Cermak, N., J. W. Becker, S. M. Knudsen, S. W. Chisholm, S. R. Manalis and M. F. Polz (2016). "Direct
568 single-cell biomass estimates for marine bacteria via Archimedes' principle." The Isme Journal **11**: 825.
569 Christie-Oleza, J. A., D. Sousoni, M. Lloyd, J. Armengaud and D. J. Scanlan (2017). "Nutrient recycling
570 facilitates long-term stability of marine microbial phototroph–heterotroph interactions." Nature
571 Microbiology **2**: 17100.
572 Coe, A., J. Ghizzoni, K. LeGault, S. Biller, S. E. Roggensack and S. W. Chisholm (2016). "Survival of
573 Prochlorococcus in extended darkness." Limnology and Oceanography **61**(4): 1375-1388.
574 de Abreu Meireles, D., J. Schripsema, A. C. Vetö Arnholdt and D. Dagnino (2015). "Persistence of Only a
575 Minute Viable Population in Chlorotic Microcystis aeruginosa PCC 7806 Cultures Obtained by Nutrient
576 Limitation." PLOS ONE **10**(7): e0133075.
577 Del Giorgio, P. A. and J. M. Gasol (2008). Physiological Structure and Single-Cell Activity in Marine
578 Bacterioplankton. Microbial Ecology of the Oceans. D. L. Kirchman.
579 Engl, C. (2018). "Noise in bacterial gene expression." Biochemical Society Transactions: BST20180500.
580 Flombaum, P., J. L. Gallegos, R. A. Gordillo, J. Rincón, L. L. Zabala, N. Jiao, D. M. Karl, W. K. W. Li, M. W.
581 Lomas, D. Veneziano, C. S. Vera, J. A. Vrugt and A. C. Martiny (2013). "Present and future global
582 distributions of the marine Cyanobacteria Prochlorococcus and Synechococcus." Proceedings of the
583 National Academy of Sciences **110**(24): 9824-9829.
584 Franklin, D. J., C. P. D. Brussaard and J. A. Berges (2006). "What is the role and nature of programmed
585 cell death in phytoplankton ecology?" European Journal of Phycology **41**(1): 1-14.
586 GILBERT, J. D. J. and W. F. FAGAN (2011). "Contrasting mechanisms of proteomic nitrogen thrift in
587 Prochlorococcus." Molecular Ecology **20**(1): 92-104.
588 Giovannoni, S. J. (2017). "SAR11 Bacteria: The Most Abundant Plankton in the Oceans." Annual Review
589 of Marine Science **9**(1): 231-255.
590 Goericke, R. and N. A. Welschmeyer (1993). "The marine prochlorophyte Prochlorococcus contributes
591 significantly to phytoplankton biomass and primary production in the Sargasso Sea." Deep Sea Research
592 Part I: Oceanographic Research Papers **40**(11): 2283-2294.
593 Grossowicz, M., D. Roth-Rosenberg, D. Aharonovich, J. Silverman, M. J. Follows and D. Sher (2017).
594 "Prochlorococcus in the lab and in silico: The importance of representing exudation." Limnology and
595 Oceanography **62**(2): 818-835.
596 Harms, A., E. Maisonneuve and K. Gerdes (2016). "Mechanisms of bacterial persistence during stress and
597 antibiotic exposure." Science **354**(6318): aaf4268.
598 Hennon, G. M. M., J. J. Morris, S. T. Haley, E. R. Zinser, A. R. Durrant, E. Entwistle, T. Dokland and S. T.
599 Dyhrman (2017). "The impact of elevated CO2 on Prochlorococcus and microbial interactions with
600 'helper' bacterium Alteromonas." The Isme Journal **12**: 520.
601 Jones, S. E. and J. T. Lennon (2010). "Dormancy contributes to the maintenance of microbial diversity."
602 Proceedings of the National Academy of Sciences **107**(13): 5881-5886.
603 Jørgensen, B. B., M. A. Lever, K. L. Rogers, K. G. Lloyd, J. Overmann, B. Schink, R. K. Thauer and T. M.
604 Hoehler (2015). "Life under extreme energy limitation: a synthesis of laboratory- and field-based
605 investigations." FEMS Microbiology Reviews **39**(5): 688-728.
606 Kashtan, N., S. E. Roggensack, S. Rodrigue, J. W. Thompson, S. J. Biller, A. Coe, H. M. Ding, P. Marttinen,
607 R. R. Malmstrom, R. Stocker, M. J. Follows, R. Stepanauskas and S. W. Chisholm (2014). "Single-Cell
608 Genomics Reveals Hundreds of Coexisting Subpopulations in Wild Prochlorococcus." Science **344**(6182):
609 416-420.

610 Klotz, A., J. Georg, L. Bučinská, S. Watanabe, V. Reimann, W. Januszewski, R. Sobotka, D. Jendrossek,
611 Wolfgang R. Hess and K. Forchhammer (2016). "Awakening of a Dormant Cyanobacterium from Nitrogen
612 Chlorosis Reveals a Genetically Determined Program." Current Biology **26**(21): 2862-2872.
613 Krumhardt, K. M., K. Callnan, K. Roache-Johnson, T. Swett, D. Robinson, E. N. Reistetter, J. K. Saunders,
614 G. Rocap and L. R. Moore (2013). "Effects of phosphorus starvation versus limitation on the marine
615 cyanobacterium Prochlorococcus MED4 I: uptake physiology." Environmental Microbiology **15**(7): 2114-
616 2128.
617 Lichtlé, C., J. C. Thomas, A. Spilar and F. Partensky (1995). "Immunological and ultrastructural
618 characterization of the photosynthetic complexes of the prochlorophyte Prochlorococcus
619 (oxychlorobacteria)." Journal of Phycology **31**(6): 934-941.
620 Ma, L., B. C. Calfee, J. J. Morris, Z. I. Johnson and E. R. Zinser (2017). "Degradation of hydrogen peroxide
621 at the ocean's surface: the influence of the microbial community on the realized thermal niche of
622 Prochlorococcus." The Isme Journal **12**: 473.
623 Malmstrom, R. R., A. Coe, G. C. Kettler, A. C. Martiny, J. Frias-Lopez, E. R. Zinser and S. W. Chisholm
624 (2010). "Temporal dynamics of Prochlorococcus ecotypes in the Atlantic and Pacific oceans." Isme J.
625 Martiny, A. C., M. L. Coleman and S. W. Chisholm (2006). "Phosphate acquisition genes in
626 Prochlorococcus ecotypes: evidence for genome-wide adaptation." Proc Natl Acad Sci U S A **103**(33):
627 12552-12557.
628 Mary, I., L. Garczarek, G. A. Tarran, C. Kolowrat, M. J. Terry, D. J. Scanlan, P. H. Burkill and M. V. Zubkov
629 (2008). "Diel rhythmicity in amino acid uptake by Prochlorococcus." Environmental Microbiology **10**(8):
630 2124-2131.
631 Matantseva, O., S. Skarlato, A. Vogts, I. Pozdnyakov, I. Liskow, H. Schubert and M. Voss (2016).
632 "Superposition of Individual Activities: Urea-Mediated Suppression of Nitrate Uptake in the
633 Dinoflagellate Prorocentrum minimum Revealed at the Population and Single-Cell Levels." Frontiers in
634 Microbiology **7**(1310).
635 Moore, L. R. and S. W. Chisholm (1999). "Photophysiology of the marine cyanobacterium
636 Prochlorococcus: Ecotypic differences among cultured isolates." Limnology and Oceanography **44**(3):
637 628-638.
638 Moore, L. R., G. Rocap and S. W. Chisholm (1998). "Physiology and molecular phylogeny of coexisting
639 Prochlorococcus ecotypes." Nature **393**(6684): 464-467.
640 Morris, J. J., R. E. Lenski and E. R. Zinser (2012). "The Black Queen Hypothesis: Evolution of
641 Dependencies through Adaptive Gene Loss." mBio **3**(2).
642 Muñoz-Marín, M. d. C., I. Luque, M. V. Zubkov, P. G. Hill, J. Diez and J. M. García-Fernández (2013).
643 "Prochlorococcus can use the Pro1404 transporter to take up glucose at nanomolar concentrations in
644 the Atlantic Ocean." Proceedings of the National Academy of Sciences **110**(21): 8597-8602.
645 Partensky, F., J. Blanchot, F. Lantoine, J. Neveux and D. Marie (1996). "Vertical structure of
646 picophytoplankton at different trophic sites of the tropical northeastern Atlantic Ocean." Deep Sea
647 Research Part I: Oceanographic Research Papers **43**(8): 1191-1213.
648 Read, R. W., P. M. Berube, S. J. Biller, I. Neveux, A. Cubillos-Ruiz, S. W. Chisholm and J. J. Grzymski
649 (2017). "Nitrogen cost minimization is promoted by structural changes in the transcriptome of N-
650 deprived Prochlorococcus cells." The ISME journal **11**(10): 2267-2278.
651 Ribalet, F., J. Swalwell, S. Clayton, V. Jiménez, S. Sudek, Y. Lin, Z. I. Johnson, A. Z. Worden and E. V.
652 Armbrust (2015). "Light-driven synchrony of Prochlorococcus growth and mortality in the subtropical
653 Pacific gyre." Proceedings of the National Academy of Sciences **112**(26): 8008-8012.
654 Rocap, G., F. W. Larimer, J. Lamerdin, S. Malfatti, P. Chain, N. A. Ahlgren, A. Arellano, M. Coleman, L.
655 Hauser, W. R. Hess, Z. I. Johnson, M. Land, D. Lindell, A. F. Post, W. Regala, M. Shah, S. L. Shaw, C.
656 Steglich, M. B. Sullivan, C. S. Ting, A. Tolonen, E. A. Webb, E. R. Zinser and S. W. Chisholm (2003).

"Genome divergence in two Prochlorococcus ecotypes reflects oceanic niche differentiation." Nature **424**(6952): 1042-1047.

Saito, M. A., M. R. McIlvin, D. M. Moran, T. J. Goepfert, G. R. DiTullio, A. F. Post and C. H. Lamborg (2014). "Multiple nutrient stresses at intersecting Pacific Ocean biomes detected by protein biomarkers." Science **345**(6201): 1173-1177.

Sauer, J., U. Schreiber, R. Schmid, U. Völker and K. Forchhammer (2001). "Nitrogen starvation-induced chlorosis in Synechococcus PCC 7942. Low-level photosynthesis as a mechanism of long-term survival." Plant Physiology **126**(1): 233-243.

Sher, D., J. W. Thompson, N. Kashtan, L. Croal and S. W. Chisholm (2011). "Response of Prochlorococcus ecotypes to co-culture with diverse marine bacteria." Isme J **5**(7): 1125-1132.

Steglich, C., M. Behrenfeld, M. Koblizek, H. Claustre, S. Penno, O. Prasil, F. Partensky and W. R. Hess (2001). "Nitrogen deprivation strongly affects Photosystem II but not phycoerythrin level in the divinyl-chlorophyll b-containing cyanobacterium Prochlorococcus marinus." Biochimica et Biophysica Acta (BBA) - Bioenergetics **1503**(3): 341-349.

Sukenik, A., I. Maldener, T. Delhaye, Y. Viner-Mozzini, D. Sela and M. Bormans (2015). "Carbon assimilation and accumulation of cyanophycin during the development of dormant cells (akinetes) in the cyanobacterium Aphanizomenon ovalisporum." Frontiers in Microbiology **6**(1067).

Szul, M. J., S. P. Dearth, S. R. Campagna and E. R. Zinser (2019). "Carbon fate and flux in *Prochlorococcus* under nitrogen limitation." mSystems **4**(1): e00254-00218.

Tamura, K., G. Stecher, D. Peterson, A. Filipski and S. Kumar (2013). "MEGA6: Molecular Evolutionary Genetics Analysis Version 6.0." Molecular Biology and Evolution **30**(12): 2725-2729.

Thompson, A. W., K. Huang, M. A. Saito and S. W. Chisholm (2011). "Transcriptome response of high- and low-light-adapted Prochlorococcus strains to changing iron availability." Isme J **5**(10): 1580-1594.

Thompson, A. W., G. van den Engh, N. A. Ahlgren, K. Kouba, S. Ward, S. T. Wilson and D. M. Karl (2018). "Dynamics of Prochlorococcus diversity and photoacclimation during short-term shifts in water column stratification at station ALOHA." Frontiers in Marine Science **5**(488).

Ting, C. S., G. Rocap, J. King and S. W. Chisholm (2002). "Cyanobacterial photosynthesis in the oceans: the origins and significance of divergent light-harvesting strategies." Trends in Microbiology **10**(3): 134-142.

Tolonen, A. C., J. Aach, D. Lindell, Z. I. Johnson, T. Rector, R. Steen, G. M. Church and S. W. Chisholm (2006). "Global gene expression of Prochlorococcus ecotypes in response to changes in nitrogen availability." Mol Syst Biol **2**: 53.

Van Mooy, B. A., G. Rocap, H. F. Fredricks, C. T. Evans and A. H. Devol (2006). "Sulfolipids dramatically decrease phosphorus demand by picocyanobacteria in oligotrophic marine environments." Proc Natl Acad Sci U S A **103**(23): 8607-8612.

Vaulot, D., D. Marie, R. J. Olson and S. W. Chisholm (1995). "Growth of Prochlorococcus, a photosynthetic prokaryote, in the equatorial Pacific Ocean." Science **268**(5216): 1480-1482.

Vila-Costa, M., R. Simó, H. Harada, J. M. Gasol, D. Slezak and R. P. Kiene (2006). "Dimethylsulfoniopropionate Uptake by Marine Phytoplankton." Science **314**(5799): 652-654.

Voigt, K., C. M. Sharma, J. Mitschke, S. Joke Lambrecht, B. Vos, W. R. Hess and C. Steglich (2014). "Comparative transcriptomics of two environmentally relevant cyanobacteria reveals unexpected transcriptome diversity." ISME J **8**(10): 2056-2068.

Yelton, A. P., S. G. Acinas, S. Sunagawa, P. Bork, C. Pedrós-Alió and S. W. Chisholm (2016). "Global genetic capacity for mixotrophy in marine picocyanobacteria." The Isme Journal **10**: 2946.

Yooseph, S., K. H. Nealson, D. B. Rusch, J. P. McCrow, C. L. Dupont, M. Kim, J. Johnson, R. Montgomery, S. Ferriera, K. Beeson, S. J. Williamson, A. Tovchigrechko, A. E. Allen, L. A. Zeigler, G. Sutton, E. Eisenstadt, Y.-H. Rogers, R. Friedman, M. Frazier and J. C. Venter (2010). "Genomic and functional adaptation in surface ocean planktonic prokaryotes." Nature **468**: 60.

Zubkov, M. V., G. A. Tarran and B. M. Fuchs (2004). "Depth related amino acid uptake by Prochlorococcus cyanobacteria in the Southern Atlantic tropical gyre." Fems Microbiology Ecology **50**(3): 153-161.

Supplementary data

Prochlorococcus rely on microbial interactions rather than on chlorotic resting stages to survive long-term stress

Dalit Roth-Rosenberg[1]#, Dikla Aharonovich[1]#, Tal Luzzatto-Knaan[1]#, Angela Vogts[2], Luca Zoccarato[3], Falk Eigemann[2], Noam Nago[1], Hans-Peter Grossart[3,4], Maren Voss[2] and Daniel Sher *[1]

[1] Department of Marine Biology, Leon H. Charney School of Marine Sciences, University of Haifa, 31905, Israel; [2] Leibniz-Institute for Baltic Sea Research, Seestrasse15, D-18119 Warnemuende, Germany; [3] Department of Experimental Limnology, Leibniz-Institute of Freshwater Ecology and Inland Fisheries, Alte Fischerhuette 2, D-16775 Stechlin, Germany; [4]Potsdam University, Institute of Biochemistry and Biology, Maulbeeralle 2, D-14469 Potsdam, Germany

* Corresponding author: dsher@univ.haifa.ac.il

# These authors contributed equally to this study

Supplementary text

Can mis-sorted cells explain the presence of non-active cells in the high-fl population, and of active cells in the low- and mid-fl populations?

FACS-sorting high-, mid- and low-fl populations from *Prochlorococcus* cultures resulted in samples that are highly enriched in the sorted populations. However, the sorted populations are not completely pure, with some incorrectly sorted cells observed when the sorted populations were re-analyzed by flow cytometry (e.g. mid- or low-fl cells in the sorted high-fl population, Supplementary Table 1). These incorrectly sorted cells could affect the interpretation of the single-cell uptake rates, for example, the presence of inactive cells in the high-fl population could be interpreted either as a real biological phenomenon (cells with high autofluorescence that are nevertheless inactive) or as the result of incorrectly sorted cells belonging to the mid- or low-fl populations (assuming the mid- and low-fl cells are inactive). To test this hypothesis, we first determined, for each cell in the NanoSIMS analysis, whether it was

753 active or inactive, defining inactive cells as those with C and N uptake rates in the range of the
754 control, i.e. glutaraldehyde killed cells (Supplementary Table 2, Killed cells C_{max} = 0.765
755 fg/cell/day and N_{max} = 0.215 fg/cell/day). We then compared the observed number of active
756 cells to the expected number of active cells, based on the number of high-, mid- and low-fl cells
757 after FACS sorting, and assuming only the high-fl cells are active. For the datasets shown in
758 Figure 2 and Supplementary Figure 3, the hypothesis that the number of active cells could be
759 explained by the number of high-fl cells after sorting was rejected (X^2 test, DF=2, $p<0.01$,
760 X^2=24.4 and n=236 cells for Figure 2, X^2=336.1 and n=415 cells for Supplementary Figure 3).
761 There were fewer active cells in the high-fl populations than expected (68% and 64% active cells
762 Supplementary Tables 2, compared to 94% and 84.5% high-fl cells, respectively, in the high-fl
763 subpopulation Supplementary Tables 1), suggesting that some high-fl cells are inactive.
764 Conversely, there were more active cells than expected in the mid- and low-fl populations (22%
765 and 51% active cells Supplementary Tables 2, compared to 7.9% and 7.5% high-fl cells,
766 respectively, in the high-fl subpopulation Supplementary Tables 1), suggesting that some cells in
767 these populations can be active.

768

769 **Estimating the fraction of *Prochlorococcus* cells living mixotrophically**

770 A rough estimate of the fraction of *Prochlorococcus* cells living mixotrophically can be obtained
771 by determining how many cells are found under conditions where the light intensity is not
772 sufficient to support active growth. We used the experimentally-determined minimal light
773 requirement for active growth of high-light and low-light adapted strains in the lab (10 μE and
774 2.8 μE during a 14:10 day-night cycle for HL and LL strains, respectively) in the lab (Moore and
775 Chisholm 1999), converting these to integrated daily PAR levels (in mole quanta m^{-2} day^{-1},
776 eMIT9313 is treated as a LL strain in this analysis despite the limited light levels analyzed for the
777 MIT9313 strain). The threshold light levels based on this calculation were 0.50 mol Q day^{-1} for
778 HL strains and 0.18 mol Q day^{-1} for LL strains. We then determined the number of
779 *Prochlorococcus* cells found at depths where the integrated daily PAR is lower than the minimal
780 light requirement (i.e. below the photic depth for *Prochlorococcus*). For this analysis, we used

781 the qPCR estimates of the cell abundance of each ecotype from a 5-year time series of the
782 *Prochlorococcus* ecotypes at the Hawaii and Bermuda time series study sites (HOT and BATS,
783 (Malmstrom et al. 2010)). In our analysis, however, we consider only the time of the year when
784 the water column is stratified (defined here as a mixed layer depth that is shallower than the HL
785 *Prochlorococcus* photic depth), because at other times cells below the photic depth but still
786 within the upper mixed layer could be mixed closer to the surface and therefore receive
787 sufficient light. During these times, the estimated photic depth for HL ecotypes was between
788 83-114m at HOT and 81-110m at BATS, and for LL ecotypes between 101-140m at HOT and
789 103-135m at BATS. An average of ~8-10% of the *Prochlorococcus* cells at HOT and BATS,
790 respectively, are found below these depths (range ~1.4-37.5% at HOT and ~0.5-43% at BATS),
791 including most of the LL cells (Supplementary Figure 7). Multiple studies have shown that
792 *Prochlorococcus* cells undergo division at these depths (growth rates of 0.1-0.2 day have been
793 recorded down to depths of 150m; e.g. (Vaulot et al. 1995, Binder et al. 1996, Liu et al. 1997)),
794 and thus at least some cells observed at these depths are not quiescent or dead. Future studies
795 are needed in order to better constrain these rough estimates of the percent of mixotrophic
796 *Prochlorococcus*, taking into account processes leading to mixing of cells below the mixed layer
797 (e.g. internal waves) and also accounting for other *Prochlorococcus* ecotypes not analyzed here.

798 **Supplementary Table 1: Cell counts and purity of the sorted cells**

		Sorted sub-populations *MIT9313 old			Sorted sub-populations **MIT9313 old		
		High	**Mid**	**Low**	**High**	**Mid**	**Low**
% Purity and number of sorted cells	**High**	3388 (94%)	239 (7.9%)	19 (1%)	3109 (84.5%)	301 (7.5%)	100 (2.9%)
	Mid	174 (4.8%)	2673 (88.2%)	172 (9.1%)	514 (14%)	3639 (91%)	685 (19.6%)
	Low	59 (1.6%)	118 (3.9%)	1699 (90%)	56 (1.5%)	57 (1.4%)	2715 (77.6%)
	Total cells	3621	3030	1890	3621	3030	1890

799 *The result refers to the experiment presented in Fig. 2

800 ** The result refers to the experiment presented in Supplementary Fig. 3

801

802

803

804

805 **Supplementary Table 2: Number of active and inactive cells in each of the sorted sub-populations.**

	Sorted sub-populations *MIT9313 old			Sorted sub-populations **MIT9313 old		
	High	**Mid**	**Low**	**High**	**Mid**	**Low**
% and number of active cells	45 (68%)	16 (22%)	3 (3.1%)	75 (64%)	107 (51%)	5 (6%)
% and number of inactive cells	21 (31.8%)	57 (78%)	94 (97%)	43 (36%)	101 (49%)	83 (94%)
Total cells	66	73	97	118	208	88

806 *The result refers to the experiment presented in Fig. 2

807 ** The result refers to the experiment presented in Supplementary Fig. 3

808

809 **Supplementary Table 3: Coefficient of variation**

Strain and growth stage	Sub-population	Illumination	Number of cells	C_{cov}	N_{cov}
Batch culture					
MIT9313, exponential growth*	High	Constant light 27 µE	158	0.92	0.89
MIT9313, old culture**	High		66	1.08-1.29	0.92-0.87
	Mid		73	2.19-2.37	1.63-1.09
	Low		97	3.77-7.11	1.83-0.85
MIT9313, old culture***	High	Photo-period 12:12 L/D, 27 µE	86	2.65	1.02
	Mid		171	5.15	0.99
	Low		73	0.69	2.33
Natural samples					
115m	High	Natural cycle approximately 14:10 L/D, 2-5 µE	55	0.73	0.16
115m	Low		45	0.61	0.33
125m	High		49	0.58	0.17
Killed cells			114	2.63	0.09

810 *The results for MIT9313 exponential growth refer to the experiment presented in Supplementary Fig.

811 5.

812 **The results for old MIT9313 cultures under constant light refer to the two experiments presented in
813 Fig. 2 and Supplementary Fig. 3.
814 *** The results for Old MIT9313 cultures under L/D refer to the experiment presented in Supplementary
815 Fig. 4.
816
817 **Supplementary figures**

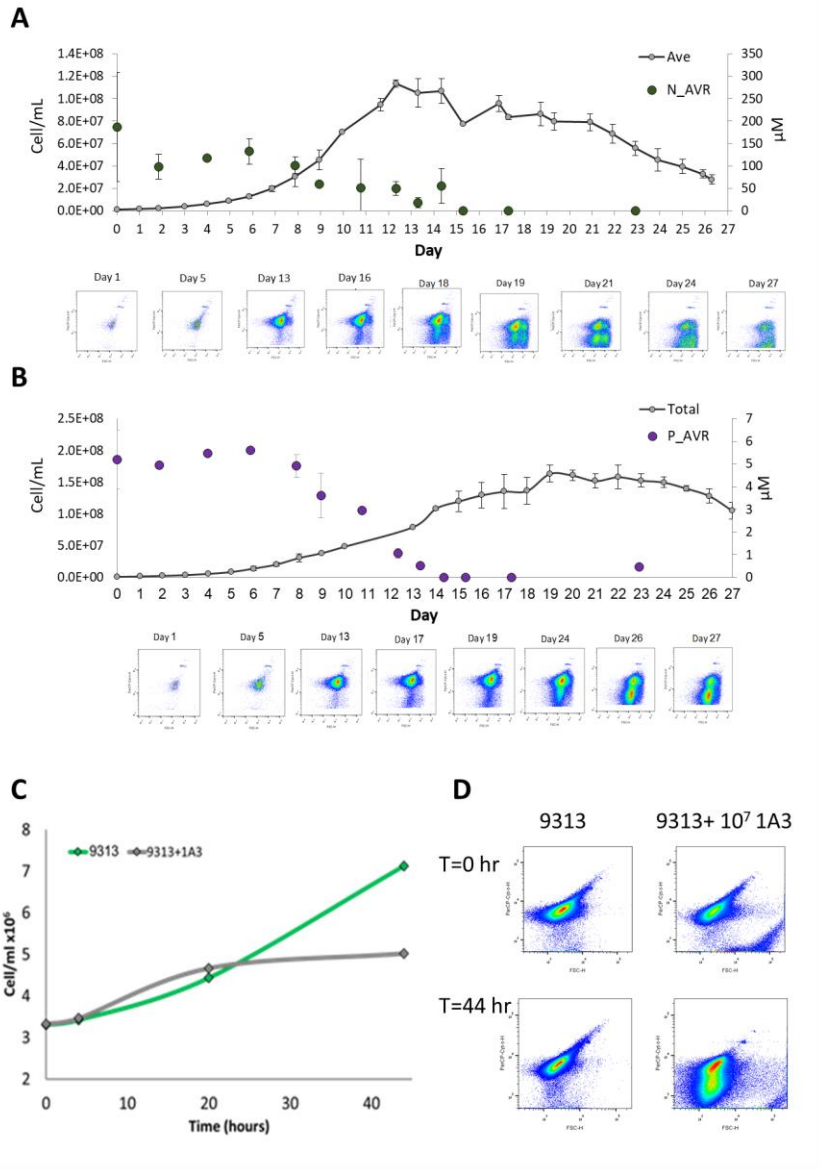

818

819 **Supplementary Figure 1:** Sub-populations of low-chl cells emerge in *Prochloroccucus* cultures under N
820 and P starvation, and when inhibited by heterotrophic bacteria. A, B) Batch cultures of strain MIT9312

821 grown under conditions where stationary phase is induced by N and P starvation (panels A and B,
822 respectively). The data shown are from (Grossowicz et al. 2017). C) Batch cultures of *Prochlorococcus*
823 MIT9313 grown axenically and in co-culture with a heterotrophic bacterium, *Alteromonas* HOT1A3. D)
824 FCM of *Prochlorococcus* populations at two time points ('0' and '44' hours). Data are from Aharonovich
825 and Sher (Aharonovich and Sher 2016).

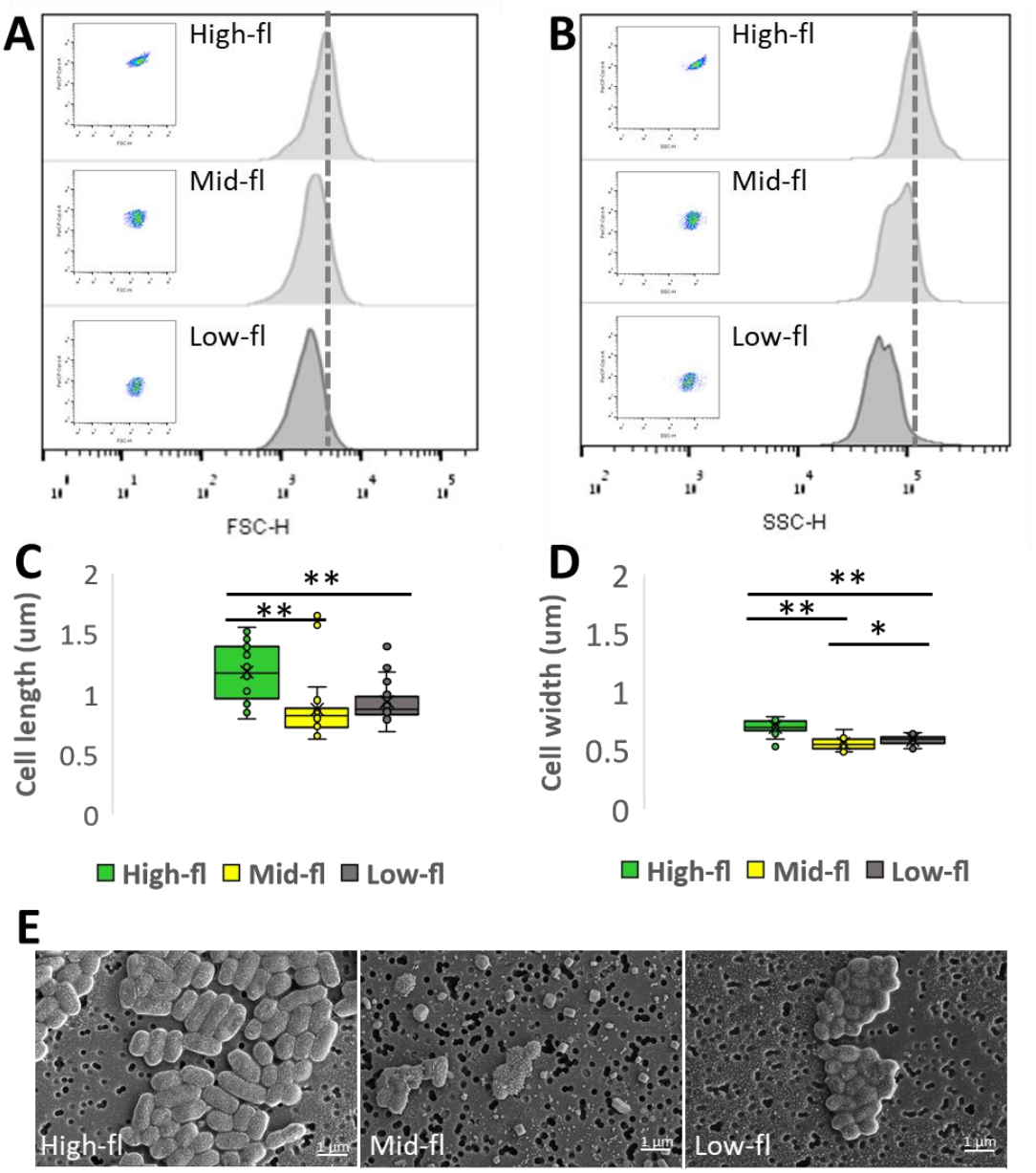

826

827 **Supplementary Figure 2: Sorted cells belonging to different sub-populations of *Prochlorococcus***
828 **MIT9313 vary in size.** A late-exponential phase MIT9313 culture was fixed using glutaraldehyde,

analyzed using flow cytometry, and the three different sub-populations sorted and observed by SEM. A, B) Histograms representing changes in cell size (Forward scatter, FSC, panel A) and complexity (Side Scatter, SSC, panel B) as measured by flow cytometry. Boxplots of variations in cell length (C) and cell width (D) as measured from SEM images of sorted populations. High-fl (n=27), Mid-fl (n=23), Low-fl (n=24). The three subpopulations were statistically different (Kruskal-Wallis test, $p<0.001$). Significant differences between each of the two populations (Mann-Whitney U test) are shown (** - $p<0.001$, * - $p<0.05$). Lengths values from Mid and Low were not significantly different. E) SEM image of sorted sub-populations, scale bar is 1um. The small square objects in the middle panel are salt crystals.

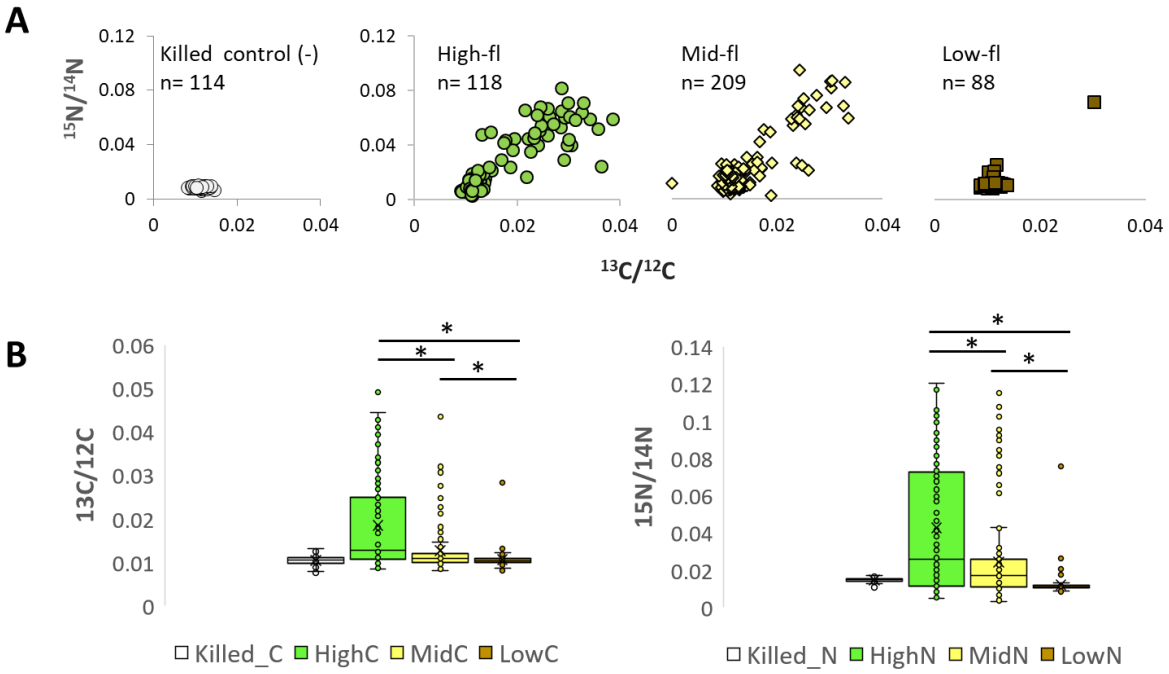

838

839

840 **Supplementary Figure 3. An independent experiment confirming differences in the metabolic activity**
841 **of sorted sub-populations of MIT9313 by NanoSIMS.** *Prochlorococcus* MIT9313 cultures were grown for
842 44 days in Pro99 and labeled with $H^{13}CO_3^-$ and $^{15}NH_4^+$ for 18h. (A) Scatterplot of $^{13}C/^{12}C$ and $^{15}N/^{14}N$ ratios
843 obtained from NanoSIMS analysis of each subpopulation (indicating the number of events detected
844 from multiple fields). (B) Boxplot represent the variances of $^{13}C/^{12}C$ and $^{15}N/^{14}N$ in each sub-population.

845 The three populations were statistically different (Kruskal-Wallis test, $p<0.001$, asterisks show significant
846 differences in comparisons between each of the two populations using the Mann-Whitney U test,
847 $p<0.001$).

848

849

850

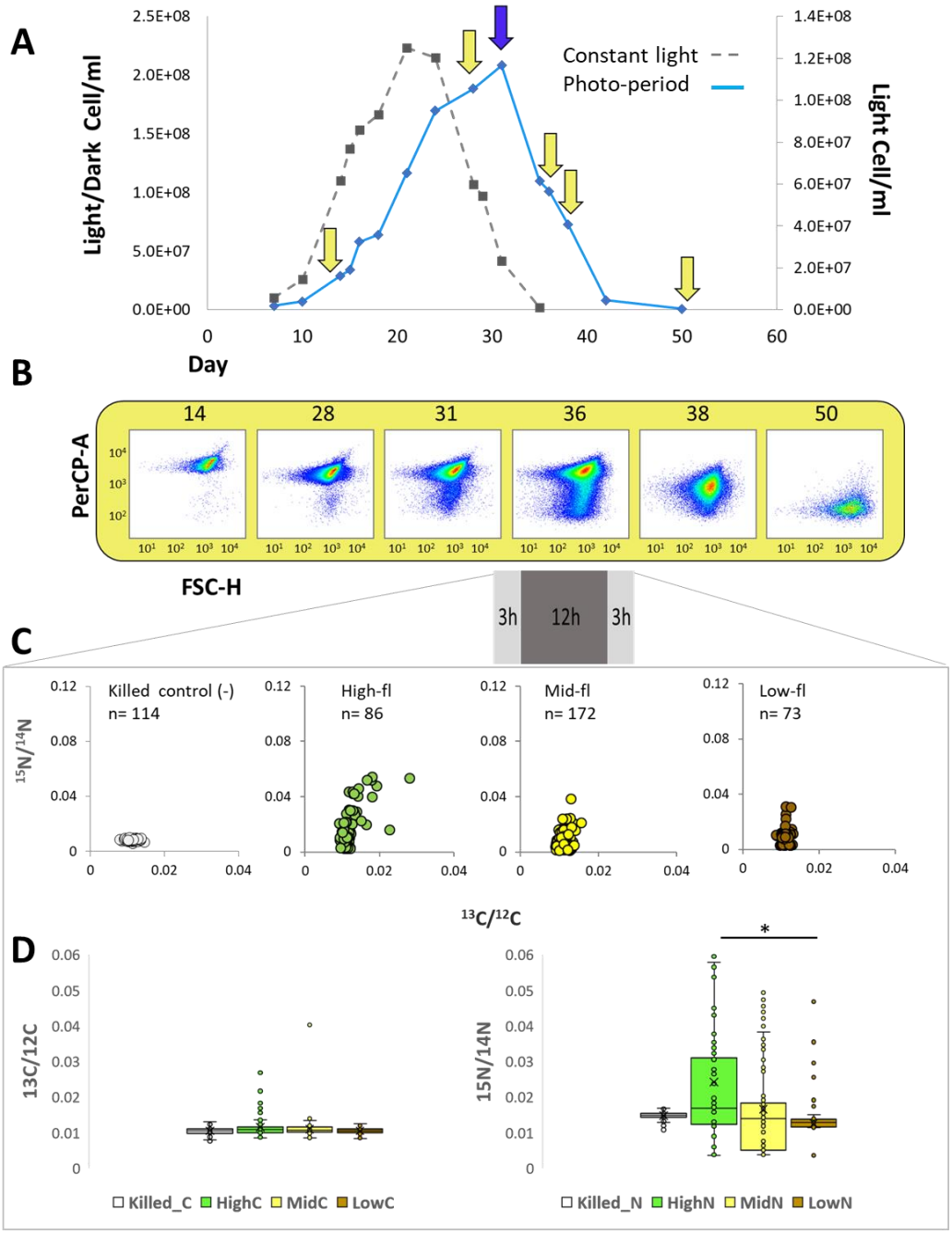

Supplementary Figure 4. NanoSIMS analysis for metabolic activity of *Prochlorococcus* chlorotic sub-populations under light/dark growth conditions. For *Prochlorococcus*, cell physiology is strongly entrained by the diel cycle, with cells typically replicating early during the night (Zinser et al. 2009). As the cultures grown for these experiments presented in Figure 2 and Supplementary Fig 3 were grown under conditions of constant light, it was possible that heterogeneity in C and N uptake rates was due to the presence of cells at different cell cycle stages. To test this hypothesis, we repeated this experiment using an MIT9313 culture grown under 12:12 light/dark conditions. The C uptake rate, as well as the cell-

878 cell heterogeneity, were lower under these conditions, potentially because the cells were in darkness for
879 12 out of the 18 hours of labeling, including the "evening" and "morning" periods when the cell's
880 photosynthetic machinery is not running at its maximal capacity (Zinser et al. 2009). In contrast, the N
881 uptake rate remained high under the light-dark cycle. This suggests that NH_4 uptake in *Prochlorococcus*
882 is decoupled from photosynthesis and occurs during both light and dark periods, unlike amino acid
883 uptake which occurs in *Prochlorococcus* primarily during the day (Mary et al. 2008). A) MIT9313 growth
884 curve under 12 h light and 12 h dark (The arrows mark the days shown in panel B.) B) A time series of
885 flow cytometry scattergrams from the tested MIT9313 culture. The x-axis is Forward Scatter (FSC, a
886 proxy for cell size), the y-axis is the chlorophyll autofluorescence of the cells. The appearance of
887 chlorotic sub-population observed from the late exponential phase (Day 31). C) Scatterplot of $^{13}C/^{12}C$
888 and $^{15}N/^{14}N$ ratios obtained from NanoSIMS analysis following 18 h incubation 3h L/12h D/3h L on day
889 36. D) Boxplot f $^{13}C/^{12}C$ and $^{15}N/^{14}N$ enrichment in each subpopulation. Glutaraldehyde killed cells used
890 as a negative control. Lines represent the median, X represents the mean, box borders are 1st quartiles
891 and whiskers represent the full range. The three populations were statistically different for N uptake
892 (Kruskal-Wallis test, $p<0.001$) but not for C uptake ($p=0.06$). Significant differences between each two
893 populations (Mann-Whitney U test) are shown (* - $p<0.001$).

894

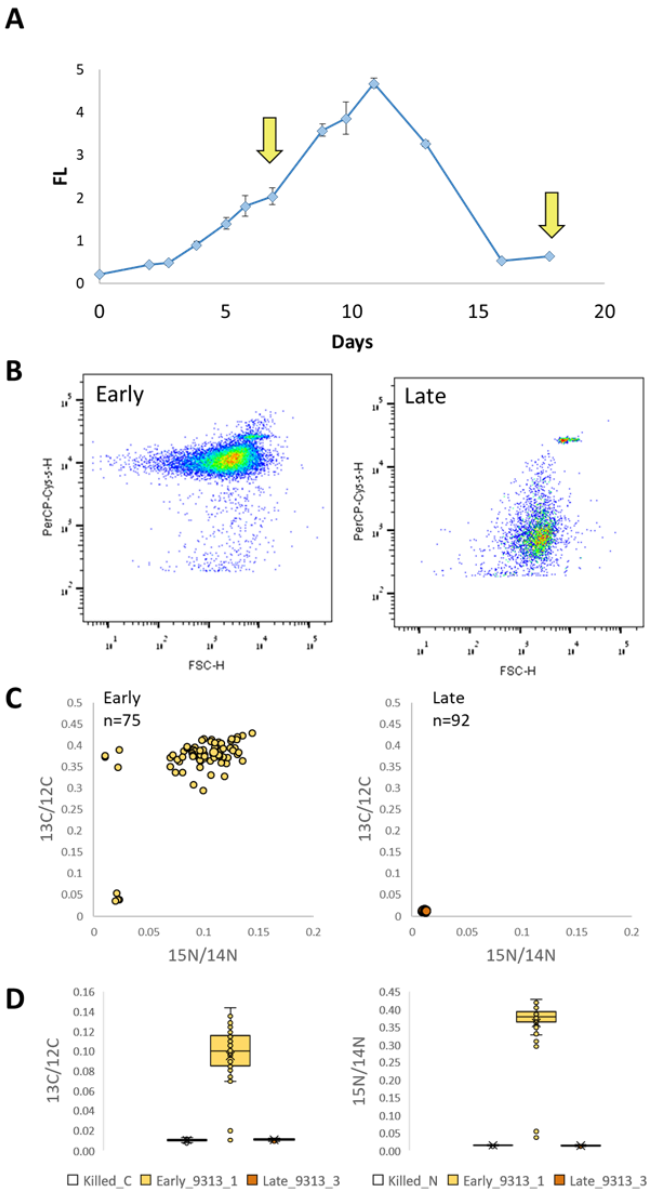

895

896

897

898

899 **Supplementary Figure 5. NanoSIMS analysis of *Prochlorococcus* MIT9313 from exponentially-growing,**

900 **nutrient-replete cultures compared to late, post-decline stage in batch culture.** We measured the N

and C uptake rates in MIT9313 cultures for which the stationary stage is induced by N starvation (low-N Pro99, N:P ratio = 2, (Grossowicz et al. 2017)). A) Growth curve monitored via the chlorophyll auto-fluorescence. Arrows indicate the heavy-nutrient labeling time points (days 7 and 18). B) FCM scatterplots of populations of 24hr post labelling. C) Scatterplot of $^{13}C/^{12}C$ and $^{15}N/^{14}N$ ratios obtained from NanoSIMS analysis, representing single cell uptake. D) Boxplot f $^{13}C/^{12}C$ and $^{15}N/^{14}N$ enrichment in each population, compared to killed cells in the control.

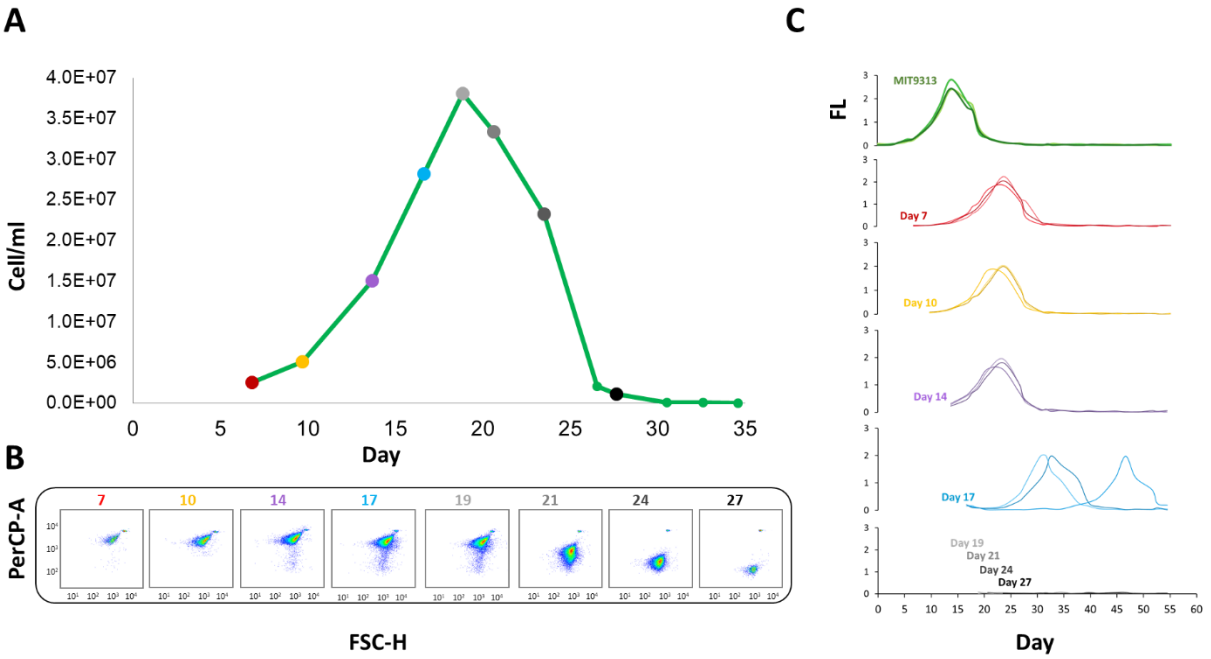

908 **Supplementary Figure 6: Time-dependent changes in viability of cells transferred into fresh media at**
909 **different life cycle stages of a batch culture. A)** A growth curve of a MIT9313 culture, under conditions
910 where stationary stage is induced by nitrogen starvation (2:1 N/P ratio in the growth media, (Grossowicz
911 et al. 2017)). Colored circles indicate the times point at which triplicate 1ml samples were transferred
912 into fresh media. B) Flow cytometry scatterplots of the culture shown in panel A. Note that, under
913 nitrogen starvation, the cultures shift rapidly from being comprised primarily of high-fl cells (day 17,
914 early stationary phase) to mainly mid-fl cells, with essentially no high-fl cells (day 21). C) Growth curves
915 of cells being transferred at different times to new, nutrient-replete media (assessed via bulk culture
916 fluorescence). Cells could not re-grow when transferred after more than 17 days of nitrogen starvation
917 suggesting that not all high-fl cells are viable, and that low-fl cells are non-viable. Similar results were
918 observed in MIT9313 cultures grown in Pro99 media, where lag phase is longer and mid-fl cells are also
919 observed (Figure 3).

920

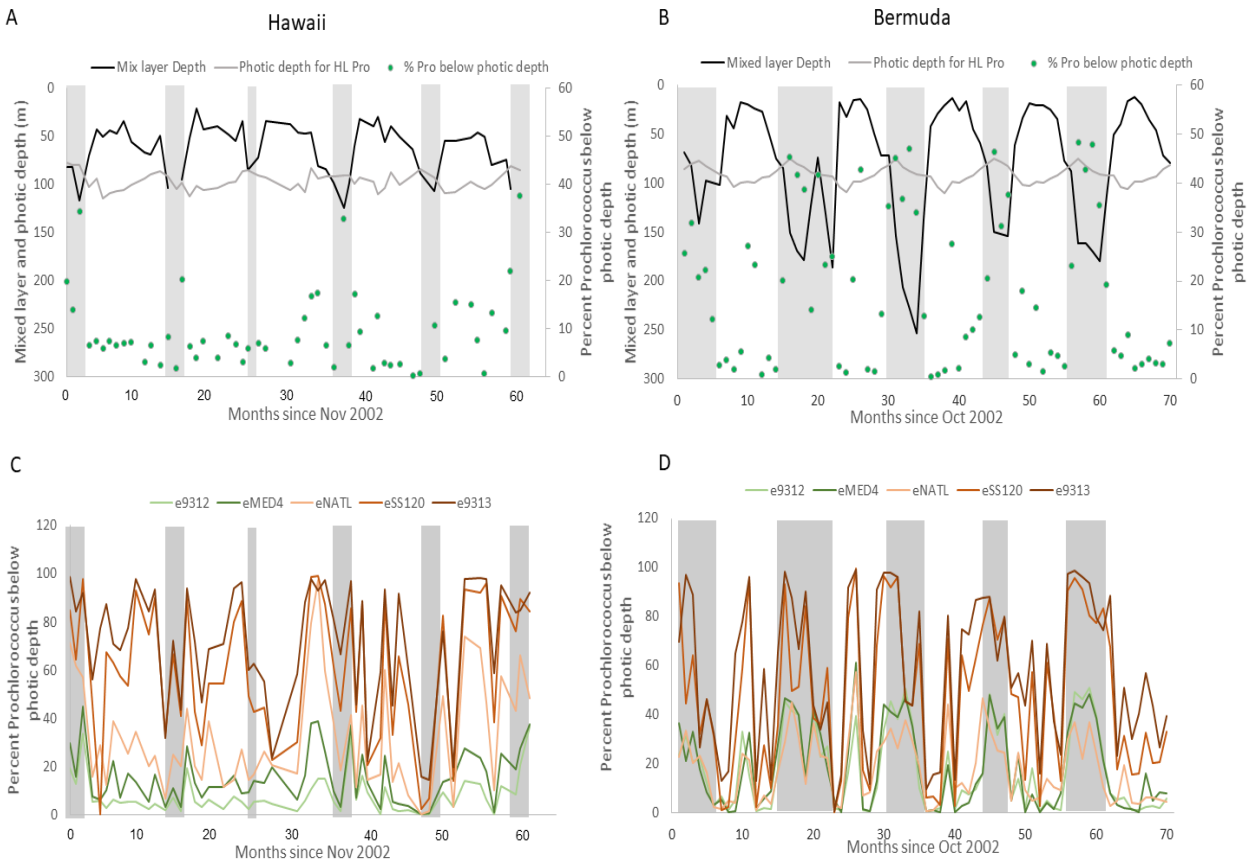

921

922 **Supplementary figure 7: Estimating the number of *Prochlorococcus* cells found below their photic zone**
923 **at Hawaii and Bermuda.** A, B) The percent of total *Prochlorococcus* cells found below their photic zone
924 at Hawaii (A) and Bermuda (B), defined as the integrated illumination level supporting the growth of
925 representative strains in laboratory cultures (Moore and Chisholm 1999) (grey line shows this depth for
926 HL strains). The black line shows the mixed layer depth (MLD), the grey areas are non-stratified
927 conditions where cells may be mixed from depth to the surface. C, D) The percentage of each
928 *Prochlorococcus* ecotype below its photic depth. For more information see supplementary text. The
929 data are taken from (Malmstrom et al. 2010).

930

931

932

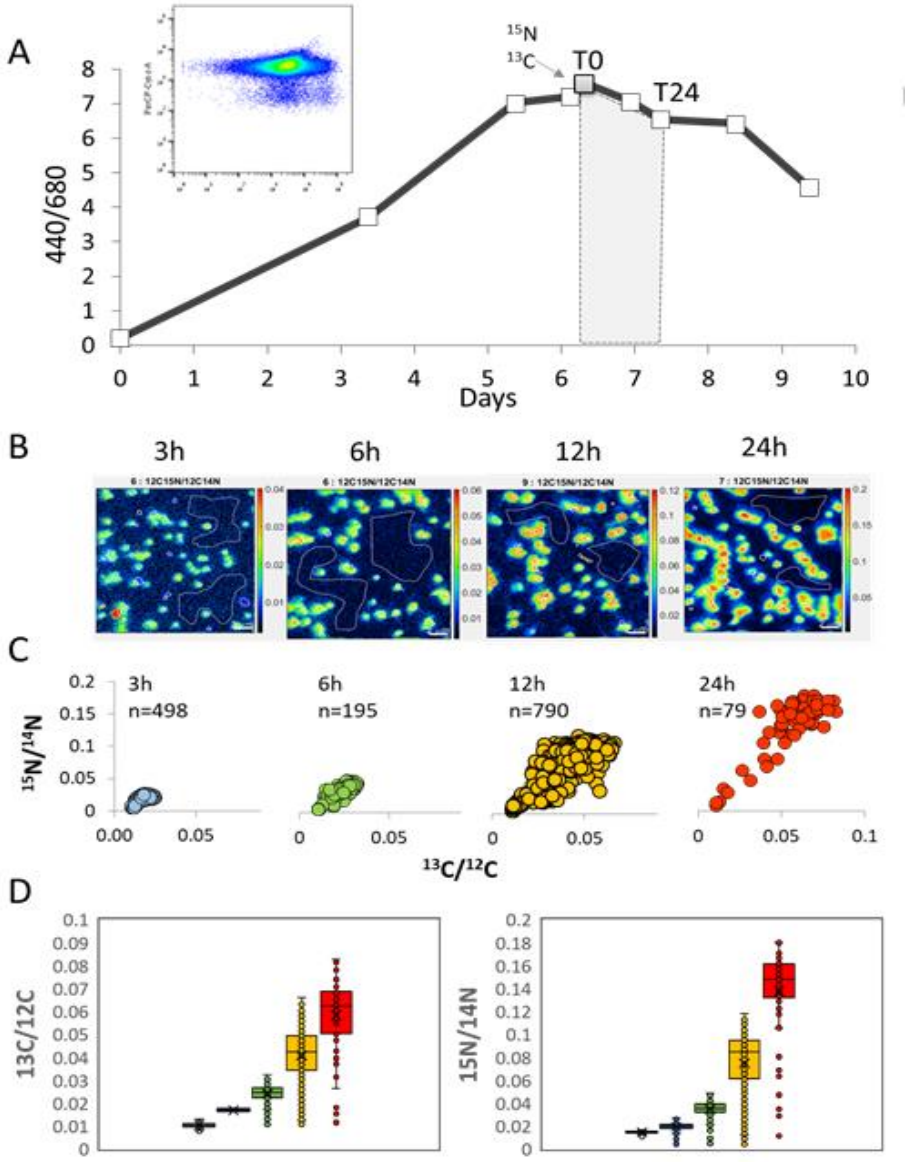

Supplementary Figure 8: Optimization for measuring metabolic activity of *Prochlorococcus* by NanoSIMS A) Growth curve of *Prochlorococcus* MED4 measured by fluorescence 440/680nm. Labeled nutrients ($H^{13}CO_3^-$ and $^{15}NH_4^+$) were added after day 6 and sampled for NanoSIMS at 3h, 6h, 12h, and 24h. Insert shows the cell population at the time of labeling (T0) by FCM. B) NanoSIMS images of $^{15}N/^{12}C$ analysis of cell for measuring metabolic activity. C) Scatterplot of $^{13}C/^{12}C$ and $^{15}N/^{14}N$ ratios obtained from NanoSIMS analysis at each time point (indicating the number of events detected from multiple fields). D) Boxplots represent the variances of $^{13}C/^{12}C$ and $^{15}N/^{14}N$ at each time point.

959 **References for supplementary information**

960 Aharonovich, D. and D. Sher (2016). "Transcriptional response of Prochlorococcus to co-culture with a
961 marine Alteromonas: differences between strains and the involvement of putative infochemicals." ISME
962 J **10**(12): 2892-2906.
963 Binder, B. J., S. W. Chisholm, R. J. Olson, S. L. Frankel and A. Z. Worden (1996). "Dynamics of
964 picophytoplankton, ultraphytoplankton and bacteria in the central equatorial Pacific." Deep Sea
965 Research Part II: Topical Studies in Oceanography **43**(4): 907-931.
966 Grossowicz, M., G. M. Marques and G. A. K. van Voorn (2017). "A dynamic energy budget (DEB) model to
967 describe population dynamics of the marine cyanobacterium Prochlorococcus marinus." Ecological
968 Modelling **359**: 320-332.
969 Grossowicz, M., D. Roth-Rosenberg, D. Aharonovich, J. Silverman, M. J. Follows and D. Sher (2017).
970 "Prochlorococcus in the lab and in silico: The importance of representing exudation." Limnology and
971 Oceanography **62**(2): 818-835.
972 Liu, H., H. A. Nolla and L. Campbell (1997). "Prochlorococcus growth rate and contribution to primary
973 production in the equatorial and subtropical North Pacific Ocean." Aquatic Microbial Ecology **12**(1): 39-
974 47.
975 Malmstrom, R. R., A. Coe, G. C. Kettler, A. C. Martiny, J. Frias-Lopez, E. R. Zinser and S. W. Chisholm
976 (2010). "Temporal dynamics of Prochlorococcus ecotypes in the Atlantic and Pacific oceans." Isme J.
977 Moore, L. R. and S. W. Chisholm (1999). "Photophysiology of the marine cyanobacterium
978 Prochlorococcus: Ecotypic differences among cultured isolates." Limnology and Oceanography **44**(3):
979 628-638.
980 Vaulot, D., D. Marie, R. J. Olson and S. W. Chisholm (1995). "Growth of prochlorococcus, a
981 photosynthetic prokaryote, in the equatorial pacific ocean." Science **268**(5216): 1480-1482.
982 Zinser, E. R., D. Lindell, Z. I. Johnson, M. E. Futschik, C. Steglich, M. L. Coleman, M. A. Wright, T. Rector, R.
983 Steen, N. McNulty, L. R. Thompson and S. W. Chisholm (2009). "Choreography of the transcriptome,
984 photophysiology, and cell cycle of a minimal photoautotroph, prochlorococcus." PLoS ONE **4**(4): e5135.

985 Agusti, S. and M. C. Sanchez (2002). "Cell viability in natural phytoplankton communities quantified by a
986 membrane permeability probe." Limnology and Oceanography **47**(3): 818-828.

987 Aharonovich, D. and D. Sher (2016). "Transcriptional response of Prochlorococcus to co-culture with a
988 marine Alteromonas: differences between strains and the involvement of putative infochemicals." ISME
989 J **10**(12): 2892-2906.
990 Bergkessel, M., D. W. Basta and D. K. Newman (2016). "The physiology of growth arrest: uniting
991 molecular and environmental microbiology." Nature Reviews Microbiology **14**: 549.
992 Berthelot, H., S. Duhamel, S. L'Helguen, J.-F. Maguer, S. Wang, I. Cetinić and N. Cassar (2018).
993 "NanoSIMS single cell analyses reveal the contrasting nitrogen sources for small phytoplankton." The
994 ISME Journal.
995 Binder, B. J., S. W. Chisholm, R. J. Olson, S. L. Frankel and A. Z. Worden (1996). "Dynamics of
996 picophytoplankton, ultraphytoplankton and bacteria in the central equatorial Pacific." Deep Sea
997 Research Part II: Topical Studies in Oceanography **43**(4): 907-931.
998 Gao, D., X. Huang and Y. Tao (2016). "A critical review of NanoSIMS in analysis of microbial metabolic
999 activities at single-cell level." Critical Reviews in Biotechnology **36**(5): 884-890.
1000 Gilbert, J. D. J. and W. F. Fagan (2011). "Contrasting mechanisms of proteomic nitrogen thrift in
1001 Prochlorococcus." Molecular Ecology **20**(1): 92-104.

Goericke, R. and N. A. Welschmeyer (1993). "The marine prochlorophyte Prochlorococcus contributes significantly to phytoplankton biomass and primary production in the Sargasso Sea." Deep Sea Research Part I: Oceanographic Research Papers **40**(11): 2283-2294.

Hughes, C., D. J. Franklin and G. Malin (2011). "Iodomethane production by two important marine cyanobacteria: Prochlorococcus marinus (CCMP 2389) and Synechococcus sp. (CCMP 2370)." Marine Chemistry **125**(1–4): 19-25.

Legendre, L. and M. Gosselin (1997). "Estimation of N or C uptake rates by phytoplankton using 15N or 13C: revisiting the usual computation formulae." Journal of Plankton Research **19**(2): 263-271.

Lennon, J. T. and S. E. Jones (2011). "Microbial seed banks: the ecological and evolutionary implications of dormancy." Nature Reviews Microbiology **9**(2): 119-130.

Llabrés, M., S. Agustí and G. J. Herndl (2011). "DIEL IN SITU PICOPHYTOPLANKTON CELL DEATH CYCLES COUPLED WITH CELL DIVISION1." Journal of Phycology **47**(6): 1247-1257.

Moore, C. M., M. M. Mills, K. R. Arrigo, I. Berman-Frank, L. Bopp, P. W. Boyd, E. D. Galbraith, R. J. Geider, C. Guieu, S. L. Jaccard, T. D. Jickells, J. La Roche, T. M. Lenton, N. M. Mahowald, E. Maranon, I. Marinov, J. K. Moore, T. Nakatsuka, A. Oschlies, M. A. Saito, T. F. Thingstad, A. Tsuda and O. Ulloa (2013). "Processes and patterns of oceanic nutrient limitation." Nature Geoscience **6**(9): 701-710.

Moore, L. R. and S. W. Chisholm (1999). "Photophysiology of the marine cyanobacterium Prochlorococcus: Ecotypic differences among cultured isolates." Limnology and Oceanography **44**(3): 628-638.

Morris, J. J., R. Kirkegaard, M. J. Szul, Z. I. Johnson and E. R. Zinser (2008). "Facilitation of robust growth of Prochlorococcus colonies and dilute liquid cultures by "helper" heterotrophic bacteria." Appl Environ Microbiol **74**(14): 4530-4534.

Muñoz-Marín, M. D. C., G. Gómez-Baena, J. Díez, R. J. Beynon, D. González-Ballester, M. V. Zubkov and J. M. García-Fernández (2017). "Glucose Uptake in Prochlorococcus: Diversity of Kinetics and Effects on the Metabolism." Frontiers in microbiology **8**: 327-327.

Muñoz-Marín, M. d. C., I. Luque, M. V. Zubkov, P. G. Hill, J. Diez and J. M. García-Fernández (2013). "Prochlorococcus can use the Pro1404 transporter to take up glucose at nanomolar concentrations in the Atlantic Ocean." Proceedings of the National Academy of Sciences **110**(21): 8597-8602.

Partensky, F., J. Blanchot, F. Lantoine, J. Neveux and D. Marie (1996). "Vertical structure of picophytoplankton at different trophic sites of the tropical northeastern Atlantic Ocean." Deep Sea Research Part I: Oceanographic Research Papers **43**(8): 1191-1213.

Read, R. W., P. M. Berube, S. J. Biller, I. Neveux, A. Cubillos-Ruiz, S. W. Chisholm and J. J. Grzymski (2017). "Nitrogen cost minimization is promoted by structural changes in the transcriptome of N-deprived Prochlorococcus cells." The ISME journal **11**(10): 2267-2278.

Ribalet, F., J. Swalwell, S. Clayton, V. Jiménez, S. Sudek, Y. Lin, Z. I. Johnson, A. Z. Worden and E. V. Armbrust (2015). "Light-driven synchrony of Prochlorococcus growth and mortality in the subtropical Pacific gyre." Proceedings of the National Academy of Sciences **112**(26): 8008-8012.

Saito, M. A., M. R. McIlvin, D. M. Moran, T. J. Goepfert, G. R. DiTullio, A. F. Post and C. H. Lamborg (2014). "Multiple nutrient stresses at intersecting Pacific Ocean biomes detected by protein biomarkers." Science **345**(6201): 1173-1177.

Sher, D., J. W. Thompson, N. Kashtan, L. Croal and S. W. Chisholm (2011). "Response of Prochlorococcus ecotypes to co-culture with diverse marine bacteria." Isme J **5**(7): 1125-1132.

Van Mooy, B. A., G. Rocap, H. F. Fredricks, C. T. Evans and A. H. Devol (2006). "Sulfolipids dramatically decrease phosphorus demand by picocyanobacteria in oligotrophic marine environments." Proc Natl Acad Sci U S A **103**(23): 8607-8612.

Vaulot, D., D. Marie, R. J. Olson and S. W. Chisholm (1995). "Growth of prochlorococcus, a photosynthetic prokaryote, in the equatorial pacific ocean." Science **268**(5216): 1480-1482.

1049 Zubkov, M. V., G. A. Tarran and B. M. Fuchs (2004). "Depth related amino acid uptake by
1050 Prochlorococcus cyanobacteria in the Southern Atlantic tropical gyre." Fems Microbiology Ecology **50**(3):
1051 153-161.

1052 Moore, L. R., G. Rocap and S. W. Chisholm (1998). "Physiology and molecular phylogeny of coexisting
1053 Prochlorococcus ecotypes." Nature **393**(6684): 464-467.

1054 Morris, J. J., R. E. Lenski and E. R. Zinser (2012). "The Black Queen Hypothesis: Evolution of
1055 Dependencies through Adaptive Gene Loss." mBio **3**(2).

1056